

1 **Re-Os geochronology and oil-source correlation of the Duvernay petroleum system,**  
2 **Western Canada sedimentary basin: Implications for the application of the Re-Os**  
3 **geochronometer to petroleum systems**

---

4 Liu, Junjie<sup>1</sup>; Selby, David<sup>1</sup>; Obermajer, Mark<sup>2</sup>; Mort, Andy<sup>2</sup>

5 <sup>1</sup>Department of Earth Sciences, Durham University, Durham, DH1 3LE, UK

6 <sup>2</sup>Geological Survey of Canada, 33rd St. NW. Calgary, Alberta, T2L 2A7, Canada

7 **Acknowledgements**

8 This research was supported by funding from a Total research award and a China Scholarship  
9 Council grant to Junjie Liu, and the Total endowment fund to David Selby. We also thank the  
10 three AAPG reviewers and the AAPG Editor, Dr. Barry J. Katz, for their constructive  
11 comments, which improved this manuscript.

12 **Abstract**

13 The rhenium-osmium (Re-Os) geochronometer has been applied to many petroleum systems  
14 worldwide. However, it is debated if the Re-Os systematics in petroleum actually records the  
15 timing of oil generation. Here, we investigate the Re-Os isotope systematics of the Duvernay  
16 petroleum system in the Western Canada sedimentary basin, which has been shown to be a  
17 relatively simple petroleum system that is associated with oil generated during the Late  
18 Cretaceous - Early Eocene Laramide orogeny from a single source.

19 The organic geochemistry of the Duvernay oils (pristane/phytane ratios of ~1.5, smooth  
20 homohopane profile,  $C_{29}>C_{27}>C_{28}$  regular sterane distribution, and predominance of  
21 diasteranes over regular steranes) strongly suggest the oil source to be that of Type I-II  
22 marine organic matter of the Late Devonian Duvernay Formation.

23 The asphaltene fraction Re-Os isotope data of the Duvernay oil yield an age of  $66 \pm 31$  Ma,  
24 which is in excellent agreement with the timing of the main-stage hydrocarbon generation of  
25 the Duvernay Formation based on basin models. Further, the similarity between the  
26  $^{187}\text{Os}/^{188}\text{Os}$  compositions of the Duvernay Formation source rock (0.46 to 1.48) and the oil  
27 (0.55 to 1.06) at the time of oil generation supports the hypothesis that the  $^{187}\text{Os}/^{188}\text{Os}$   
28 composition of an oil is inherited from the source unit at the time of oil generation, and  
29 therefore shows no, or limited influence from interaction with basin fluids. This study  
30 supports that the Re-Os isotope systematics of an oil can yield the timing of oil generation,  
31 and be used to trace its source.

## 32 **1. Introduction**

33 Establishing an accurate and precise age of hydrocarbon generation is crucial for  
34 understanding the evolution of a petroleum system. Timing constraints for hydrocarbon  
35 generation can be achieved through many techniques, for example, basin modelling with  
36 paleotemperature and petroleum generation kinetics; or the timing of oil generation can be  
37 inferred by constraining the earliest migration of oil using radiometric dating ( $^{40}\text{Ar}/^{39}\text{Ar}$ ) of  
38 fluid inclusions and diagenetic minerals, e.g., authigenic illite and K-feldspar (Eadington et

39 al., 1991; Kelly, 2002; Mark et al., 2005; Mark et al., 2010; Welte et al., 2012). Despite the  
40 contribution of these methods to the understanding of petroleum system evolution, they are  
41 limited by poorly constrained parameters (e.g., paleogeothermal gradient) or difficulties  
42 associated with sampling and analyzing (e.g., grain size versus purity of authigenic minerals  
43 for radiometric dating). During the past decade, the rhenium-osmium (Re-Os) chronometer  
44 has been demonstrated to be a promising radiometric tool to directly date petroleum samples  
45 and for oil-source correlation (Selby and Creaser, 2005b; Selby and Creaser, 2005a; Selby et  
46 al., 2007; Finlay et al., 2011; Finlay et al., 2012; Rooney et al., 2012; Lillis and Selby, 2013;  
47 Cumming et al., 2014; Ge et al., 2017).

48 Rhenium-Os analysis demonstrating chronologic information in petroleum systems was first  
49 shown by Selby et al. (2005), who derived a Re-Os date of  $374.2 \pm 8.6$  Ma (MSWD = 11.7,  
50 Model 3) for bitumen formation in the Polaris Mississippi Valley Type deposit, Nunavut,  
51 Canada, which is in agreement with contemporaneous Pb-Zn mineralization dated at  $366 \pm 15$   
52 Ma (Rb-Sr sphalerite methodology). In addition, Re-Os data derived from highly biodegraded  
53 oil from the Oil Sand deposits of Alberta, Canada, give an age of  $111.6 \pm 5.3$  Ma (MSWD =  
54 2.2, Model 3) (Selby and Creaser, 2005a), which is in agreement with the basin model of  
55 Riediger et al. (2001). Consequently, the Re-Os date is taken to record the timing of oil  
56 generation and migration in the world's largest oil sand system. However, the Re-Os age for  
57 the oil sands is inconsistent with some other basin models proposed for this complex oil  
58 system, e.g. Higley et al. (2009), Berbesi et al. (2012), and a recent study on trap restoration

59 and the bitumen present in kimberlites (Tozer et al., 2014) which could relate to secondary  
60 migration of oil in the Alberta basin.

61 Oil Re-Os dates ( $68 \pm 13$  Ma) from the UK Atlantic Margin (UKAM) petroleum system  
62 (Finlay et al., 2011) also correspond to the age of petroleum generation determined through  
63 basin modelling (Lamers and Carmichael, 1999) and K-feldspar cement  $^{40}\text{Ar}/^{39}\text{Ar}$  dating  
64 (Mark et al., 2005). A Re-Os study of oils from the Phosphoria petroleum system, Bighorn  
65 basin, USA produced an age of  $211 \pm 21$  Ma, corresponding to the start of petroleum  
66 generation according to basin modelling rather than the re-migration of oil (during the  
67 Laramide orogeny which starts from 80 - 70 Ma and ended until 55 - 35 Ma, although the  
68 exact dates are in dispute; English and Stephen, 2004) or the deposition of the source rock  
69 (during the Permian,  $\sim 270$  Ma) (Lillis and Selby, 2013). Although the UKAM and  
70 Phosphoria oils are variably biodegraded, the process has not appreciably disturbed the Re-  
71 Os systematics from recording the timing of generation of oil. This is supported by the fact  
72 that Re and Os in oil are hosted predominantly by the asphaltene fraction (Selby et al., 2007),  
73 which is the most resistant phase to biodegradation (Wenger et al., 2001; Peters et al., 2005).  
74 More recently, Re-Os bitumen data has provided insights into the temporal hydrocarbon  
75 evolution in the Longmen Shan Thrust Belt, southwest China, i.e. the multiple oil generation  
76 episodes (486 Ma and 172 - 162 Ma) and sources, and its relationship to tectonism, and  
77 additionally discussed implications for future exploration of the adjacent petroliferous  
78 Sichuan Basin (Ge et al., 2017). Furthermore, a study of the Green River petroleum system in  
79 the Uinta basin, USA, demonstrated the capacity of the Re-Os chronometer to yield the

80 timing of oil generation ( $19 \pm 14$  Ma) in lacustrine petroleum systems in addition to marine  
81 petroleum systems (Cumming et al., 2014).

82 Unlike previous studies using multiple oil and/or bitumen samples to establish a Re-Os date,  
83 a study focusing on two oil families of the Gela oil field, southern Sicily, Italy, which are  
84 sourced from the Noto Formation (Upper Triassic, Rhaetian) and the Streppenosa Formation  
85 (Lower Jurassic, Hettangian), respectively, promotes the establishment of Re-Os dates using  
86 fractions of one single oil sample, in order to negate possible disadvantages of using multiple  
87 oil samples from a wide geographic region (Georgiev et al., 2016). The authors analysed the  
88 asphaltene and maltene fractions, which were separated using a series of solvents (*n*-pentane,  
89 *n*-hexane, *n*-heptane and *n*-decane). The best-fit lines of the Re-Os data for asphaltenes from  
90 one oil family and for maltenes from the other oil family yield reasonable oil generation ages  
91 for each family ( $27.5 \pm 4.6$  Ma and  $200.0 \pm 5.2$  Ma, respectively). However, this approach of  
92 obtaining a Re-Os oil generation age from one single oil sample is potentially confined to oils  
93 with high asphaltene contents and Re and Os abundances. It also depends on the difference of  
94 asphaltenes and maltenes separated by different *n*-alkanes from the same oil to obtain a range  
95 in Re-Os isotopic compositions sufficient to obtain an isochron. As such, oils with low Re  
96 and Os abundances will be too analytically challenging to obtain precise data to distinguish  
97 these differences.

98 Hydrous pyrolysis experiments on organic-rich sedimentary rocks (Rooney et al., 2012;  
99 Cumming et al., 2014) have shown that during thermal maturation, Re and Os will be

100 transferred to the generated oil, although the majority of the Re and Os remains in the source  
101 rock. The  $^{187}\text{Re}/^{188}\text{Os}$  values show no consistent relationship between the source rock and the  
102 generated oil, but the  $^{187}\text{Os}/^{188}\text{Os}$  composition of a source rock is inherited by the generated  
103 oil (Selby et al., 2005; Finlay et al., 2011; Rooney et al., 2012; Cumming et al., 2014). The  
104 relationship between the  $^{187}\text{Os}/^{188}\text{Os}$  composition of a source rock and the  $^{187}\text{Os}/^{188}\text{Os}$   
105 composition of the generated oil (at the time of generation) is employed in the  
106 aforementioned studies for oil-source correlation. For example, the attempt of identifying the  
107 source(s) for the Polaris bitumen through the Os isotope composition of a few Phanerozoic  
108 and Proterozoic potential source rocks led to the conclusion of the mix of several source  
109 rocks or a main source unit that was not sampled in the study for the studied bitumen. In  
110 addition, the coupling of Pt/Pd values with  $^{187}\text{Os}/^{188}\text{Os}$  compositions has been employed as a  
111 viable inorganic oil-source correlation tool in recognizing the Lower Jurassic Gordondale  
112 Member as the predominant source of the Canadian oil sands (Finlay et al., 2012), which is  
113 supported by basin and migration modelling studies (Higley et al., 2009; Berbesi et al., 2012).

114 Although present studies show that biodegradation has little influence on the Re-Os  
115 systematics of asphaltene (Selby and Creaser, 2005a; Selby et al., 2005; Finlay et al., 2012;  
116 2014), they can be vulnerable to other secondary alteration processes of petroleum. For  
117 example, disturbance of the Re-Os systematics has been shown for oils spatially associated  
118 with the main basin-bounding faults of the Viking Graben and East Shetland basin of the  
119 North Sea, United Kingdom (Finlay et al., 2010). Here, oils are suggested to have been  
120 contaminated by fault-charged mantle-fluids that contain Os with a non-radiogenic

121  $^{187}\text{Os}/^{188}\text{Os}$  composition. As a result, the Re-Os systematics of the oil fail to yield a  
122 generation age, but instead trace the crustal-scale fluid dynamics and migration. Such  
123 processes have also been demonstrated in the laboratory, where experiments have shown that  
124 Re and Os in aqueous phase can transfer into oil during oil-water contact under various  
125 conditions (Mahdaoui et al., 2015). Thermal cracking may also reset the Re–Os isotope  
126 systematics in petroleum and result in only the timing of thermal cracking and generation of  
127 dry gas and pyrobitumen being recorded (Lillis and Selby, 2013; Ge et al., 2016). Similarly,  
128 thermochemical sulphate reduction (TSR) of oil may also disturb or even reset the Re-Os  
129 systematics in oil. For example, the Re-Os data from oils affected by TSR in the Big Horn  
130 basin yield a Re-Os date of  $9.24 \pm 0.39$  Ma, which is in agreement with the proposed end of  
131 TSR as a result of reservoir cooling due to the major uplift and erosion at  $\sim 10$  Ma (Lillis and  
132 Selby, 2013).

133 The previous attempts and achievements of using Re-Os as petroleum generation  
134 geochronometer and oil-source tracer are often compromised by the lack of understanding, or  
135 intrinsic complex geological characteristics, of the petroleum systems. The source units of  
136 some petroleum systems are often debated or represent mixed sources. For example: 1) the  
137 Phosphoria system records a mixed oil generated from two separate members of the Permian  
138 Phosphoria Formation, i.e. Meade Peak Member (ca. 270 Ma) and Retort Member (ca. 265  
139 Ma), which have an age difference of about 5 million years; 2) the Eocene Green River  
140 Formation (ca. 52 to 44 Ma) is over 3000 m (10000 ft) thick, within which many members  
141 are considered as possible oil sources (Anders et al., 1992; Ruble et al., 2001); 3) the

142 Canadian Oil Sands may have a mixed source, although the main contributor is highly  
143 debated (Riediger et al., 2001; Higley et al., 2009; Berbesi et al., 2012; Finlay et al., 2012;  
144 Adams et al., 2013). Inconsistent thermal maturation timings, multiple stages of oil  
145 generation and remigration are also often proposed by geological models. Both multiple  
146 sources and multiple stages, or prolonged oil generation, are likely to yield a large range of  
147 initial  $^{187}\text{Os}/^{188}\text{Os}$  compositions of generated oil. Some oil samples are also altered (e.g.,  
148 biodegradation, thermal cracking, and thermochemical sulphate reduction), for which the  
149 possibility and degree of disturbance to the oil Re-Os systematics has been discussed, but not  
150 yet fully understood. Further, the application of the  $^{187}\text{Os}/^{188}\text{Os}$  composition as an oil-source  
151 correlation tool suffers from the lack of source rock Re-Os data in many cases. For example,  
152 the Green River Formation is over 3000 m (10000 ft) thick, but the shale samples for Re-Os  
153 dating were collected from three intervals with most of the samples spanning only 1 to 3 m (3  
154 to 10 ft) (Cumming et al., 2014).

155 Here, as an examination of the usefulness of the application of the Re-Os chronometer in  
156 petroleum systems, we present the study on the simple and well-characterized Duvernay  
157 petroleum system of the Western Canada sedimentary basin (WCSB). The oil in this  
158 petroleum system is sourced from the Late Devonian Duvernay carbonaceous shale (Stoakes  
159 and Creaney, 1984; Li et al., 1998; Fowler et al., 2001). Oil generation from the Late  
160 Devonian Duvernay carbonaceous shale occurred during the Late Cretaceous to Eocene,  
161 associated with the Laramide orogeny (Deroo et al., 1977; Creaney and Allan, 1990). The  
162 generated oil migrated into the adjacent Leduc reef build-ups in the Rimbey-Meadowbrook

163 reef chain and Bashaw reef complex area, and then into the overlying Winterburn Group  
164 Nisku Formation (Creaney et al., 1994; Rostron, 1997). Biomarker analyses indicate that the  
165 Duvernay Formation is the only source of this petroleum system and that crude oil has  
166 experienced limited secondary alteration (Li et al., 1998; Fowler et al., 2001). We present Re-  
167 Os data from oil and source units, coupled with organic geochemistry, and discuss the  
168 geochronology and oil-source correlation of the Duvernay petroleum system and the  
169 implications for the application of the Re-Os geochronometer to petroleum systems.

## 170 **2. Geological setting**

171 The Duvernay petroleum system is located in south-central Alberta within the Western  
172 Canada sedimentary basin (Fig. 1). The Late Devonian Woodbend and Winterburn strata in  
173 the basin represent a thick and lithologically complex accumulation of shales and carbonates  
174 (Fig. 2). The two salient features of the Woodbend and Winterburn strata are the high quality  
175 source rocks and reservoirs they encompass, for example, the prolific Duvernay  
176 Formation and the porous carbonates of the Leduc and Nisku Formations.

177 The Late Devonian Duvernay Formation of the Woodbend Group was deposited as marine  
178 basin-filling laminated carbonates and shales (Stoakes and Creaney, 1984; Switzer et al.,  
179 1994; Chow et al., 1995; Fowler et al., 2001; Fothergill, 2014). The Duvernay Formation  
180 correlates with the Muskwa Formation to the north, and the Horn River and Canol  
181 Formations in the Northwest Territories. The formation also overlies the platform carbonates  
182 of the Cooking Lake Formation and is in turn overlain by the basin-filling calcareous shales

183 of the Ireton Formation. The thickness varies depending on proximity to Devonian reef build-  
184 ups and is predominantly 20 - 60 m (60 to 200 ft) (Fig. 17, Switzer et al., 1994; Fothergill,  
185 2014), but is up to 90 m (300 ft) within some carbonate embayments adjacent to the Killam  
186 Barrier reef-edge (Switzer et al., 1994; Fowler et al., 2001). The organic matter is  
187 concentrated in thin (typically a few mm) alternating laminae within the Duvernay  
188 Formation, which are separated by an organic-poor mudstone. Petrographically, the laminates  
189 of the Duvernay Formation contain abundant algalite macerals and some bituminite, often  
190 within an amorphous organic matrix, indicating that they represent periods of significant  
191 accumulation and preservation of oil-prone Type II marine organic matter (Fowler et al.,  
192 2001). This organic-poor mudstone becomes thinner (30 m (100 ft)) in the center of the basin  
193 (Switzer et al., 1994) to the west and reduces the separation between the two organic-rich  
194 intervals (Chow et al., 1995). The average TOC content ranges from 4 wt.% to 6 wt.%,  
195 although occasionally it is as high as 17 wt. % (Stoakes and Creaney, 1984; Chow et al.,  
196 1995; Higley et al., 2009; Dunn et al., 2012).

197 The numerous isolated Leduc reef build-ups (e.g., Rimbey-Leduc-Meadowbrook chain,  
198 Redwater, Bashaw) sit stratigraphically above the Cooking Lake and Beaverhill Lake  
199 Formations and partially interfinger with the Duvernay Formation (Fig. 1 - 2). The Leduc  
200 reefs are up to 275 m (900 ft) thick (Switzer et al., 1994; Chow et al., 1995; Rostron, 1997)  
201 and are highly porous and permeable (Amthor et al., 1994). A broad Leduc carbonate shelf  
202 also developed on the Cooking Lake Formation to the southeast of the basin. The Winterburn  
203 Nisku Formation is dominated by an extensive carbonate shelf in the East Shale basin to the

204 east of the Rimbey-Meadowbrook Leduc reef trend. Its thickness decreases from 60 m (200  
205 ft) near the underlying Leduc reef trend to about 20 m (60 ft) in the east, with its lithology  
206 changing stratigraphically from interbedded shale and limestone to relatively pure carbonates  
207 (Switzer et al., 1994).

208 The hydrocarbon maturation of the majority of the Phanerozoic strata of the WCSB did not  
209 occur until the Laramide orogeny (Late Cretaceous-Eocene) and was terminated by  
210 subsequent uplift and erosion (Deroo et al., 1977; Creaney and Allan, 1990; Bustin, 1991). As  
211 a result of the eastward propagation of crustal down-warping and foreland basin  
212 development, deep burial and thermal maturation progressed from the foreland belt  
213 northeastward across the plain. Present day isomaturity maps of Jurassic and younger source  
214 rocks (Bustin, 1991) display a decrease in thermal maturity from the foredeep to the  
215 shallower part of the basin in the northeast, where significant hydrocarbon generation  
216 occurred until the Eocene. Also estimated by apatite fission track studies (Issler et al., 1999),  
217 the peak paleo-temperature and inferred maximum burial depth is estimated from apatite  
218 fission track dating to have occurred at ~ 60 Ma.

219 It is generally accepted that the Duvernay source rocks have generated large amounts of  
220 hydrocarbons, with volume estimations ranging up to 100 million barrels (MMbbl) per square  
221 mile (39 MMbbl per square kilometre; Jenden and Monnier, 1997). The generated oil  
222 migrated extensively both laterally and stratigraphically within the basin, including in the  
223 older Beaverhill Lake and Elk Point reservoirs. But migration of oils was largely confined to

224 the Cooking Lake-Leduc and Nisku Formations by the low permeability shales, dolomitic  
225 carbonates and anhydrites of the Devonian Waterways Formation, Ireton Formation and  
226 Wabamun Group (Fig. 3; Stoakes and Creaney, 1985; Creaney and Allan, 1990; Rostron,  
227 1997) over most of central and northern Alberta. The generated oil migrated locally into the  
228 Cooking Lake platform margins and Leduc reefs (Rimbey-Meadowbrook trend and Bashaw  
229 Reefs), and the stratigraphically older Beaverhill Lake platform present in an updip position  
230 due to the regional tilt of the strata (Fig. 31, Creaney and Allan, 1992; Creaney et al., 1994;  
231 Fig. 5, Rostron, 1997). The Cooking Lake Formation also provided a migration pathway for  
232 the isolated Leduc reef as a "leaky pipeline" dependent on the local presence or absence of  
233 permeability barriers (Stoakes and Creaney, 1984). The Ireton shale serves as the seal to the  
234 Duvernay petroleum system. However, due to the absence or the thin nature of the Ireton  
235 shale in some places, oil also leaked into the overlying Nisku carbonates in the Bashaw area  
236 (Rostron, 1997; Li et al., 1998). Geochemical studies (Creaney et al., 1994; Li et al., 1998;  
237 Fowler et al., 2001) documented that the organic geochemical composition of the Duvernay  
238 Formation extracts is quite similar to most of the crude oils found within the Leduc-Nisku  
239 intervals along the Rimbey-Meadowbrook and Bashaw reef trends. In fact, geochemical oil-  
240 source correlations have demonstrated that the Leduc and Nisku oils are almost all sourced  
241 from the Duvernay Formation with probably only a very small contribution of the Nisku  
242 source to the Nisku oils (Rostron, 1997; Li et al., 1998; Harris et al., 2003).

243 Gas chromatography and biomarker data show that there is no or limited alteration of the  
244 Leduc and Nisku oils by biodegradation or water washing. Thermal cracking and

245 thermochemical sulphate reduction of crude oil occurred only in the foredeep (Evans et al.,  
246 1971; Rogers et al., 1974; Creaney and Allan, 1992; Marquez, 1994; Stasiuk, 1997; Fowler et  
247 al., 2001). The generated gas migrated up-dip and may have resulted in deasphalting, which  
248 is considered responsible for the high H<sub>2</sub>S content of some of the stratigraphically-higher  
249 crude oil (Simpson, 1999; Fowler et al., 2001).

### 250 **3. Sample preparation and analysis methodology**

#### 251 **3.1 Oil samples**

252 All oil samples analysed in this study were taken from the oil library of the Geological  
253 Survey of Canada - Calgary office (GSC-C). The selected oils are from both the Leduc and  
254 Nisku reservoirs in the area of the Rimbey-Meadowbrook Leduc reef trend and the Bashaw  
255 reef complex between Edmonton and Calgary (Fig. 1; Table 1). Prior to sampling, the  
256 archived oil was thoroughly mixed to remove any density separation of oil fractions that had  
257 occurred during storage.

258 The selected Duvernay oil samples typically have low asphaltene contents. Given that Re and  
259 Os are both predominantly present in the asphaltene fraction, and that the Re–Os isotopic  
260 composition of an asphaltene can be used as an approximation for that of the bulk oil (Selby  
261 et al., 2007), the asphaltene fractions were separated from the oils to permit more precise  
262 determinations of the Re and Os isotope compositions. The separation of asphaltene from the  
263 bulk oil follows the principles and steps outlined by Speight (2004) and Selby et al. (2007).  
264 For each gram of crude oil, 40 ml of *n*-heptane (or *n*-pentane) was added, and the mixture

265 was agitated on a rocker overnight (~ 20 h) at room temperature. Asphaltene is the insoluble  
266 fraction of oil in *n*-heptane (or *n*-pentane) and was isolated from the maltene-bearing *n*-  
267 heptane (or *n*-pentane) fraction by centrifuging at 3500 rpm for 15 minutes. Following the  
268 removal of the *n*-heptane (or *n*-pentane), the asphaltene was extracted using chloroform and  
269 dried at 60°C.

### 270 **3.2 Source rock**

271 In addition to the Duvernay oil asphaltene, the organic-rich Duvernay Formation was also  
272 analysed for its Re and Os abundances and Re-Os isotopic composition. The shale and  
273 carbonaceous shale samples of the Duvernay Formation were collected from the cores of  
274 wells 16-18-52-5W5, 14-29-48-6W5, 2-6-47-4W5 and 10-27-57-21W4 (Fig. 1; Table 2). The  
275 Re-Os data from these samples were compiled with previously published Re-Os data from  
276 the Duvernay Formation from wells 2-12-50-26W4, 8-35-31-25W4 and 1-28-36-3W5 (Selby  
277 et al., 2007; Finlay et al., 2012). The entire sample set covers a large geographical area of 300  
278 × 150 km<sup>2</sup> (1866 × 93 sq mi). As a result, the sample set, with respect to hydrocarbon  
279 maturation, ranges from immature to highly mature with an average R<sub>o</sub> from 0.5 % of 10-27-  
280 57-21W4 to 1.25 % of 2-6-47-4W5 and 1.45 % of 1-28-36-3W5 (Stasiuk and Fowler, 2002),  
281 and possesses highly variable TOC contents (from less than 1 wt.% to over 10 wt.%).

282 Depending on the thickness of the Duvernay Formation interval of each well, most samples  
283 were taken equally from each well at 0.5 m (1.6 ft; 16-18-52-5W5, ~1.5 m (4.9 ft)) and 2 m  
284 (7 ft; 14-29-48-6W5, ~8 m (26 ft); 2-6-47-4W5, ~20 m (60 ft)) or as equal as possible

285 depending on availability (10-27-57-21W4) in order to obtain a Re-Os data set that was  
286 representative of the entire Duvernay Formation organic-rich interval (Table 2). The collected  
287 core samples were cut and polished to remove any drilling marks and materials, and dried at  
288 60°C. Approximately 30 g of rock for each sample was crushed to a fine homogeneous  
289 powder using a Zr dish.

### 290 **3.3 Organic geochemical analyses**

291 All geochemical analyses were performed at the organic geochemistry laboratory of the  
292 Geological Survey of Canada - Calgary office. Pyrolysis of pulverized rock samples was  
293 carried out using Delsi Rock-Eval II and Rock-Eval 6 instruments (for measurement details  
294 see Espitalie et al., 1985; Behar et al., 2001). Biomarker analyses were performed on low- to  
295 high-maturity Duvernay sourced oil samples and source rock solvent extracts. Soluble  
296 organic matter was extracted from powdered rock samples of the Duvernay Formation for 24  
297 hours using a chloroform:methanol (87:13) mixture. The extracts and crude oils were treated  
298 with approximately 40 volumes of *n*-pentane to precipitate the asphaltenes. The deasphalted  
299 extracts and oils were fractionated using open column chromatography. Saturates were  
300 recovered by eluting with pentane, aromatics by eluting with a 50:50 mixture of pentane-  
301 dichloromethane, and resins were recovered with methanol.

302 The gasoline range fractions (*i*-C<sub>5</sub>-*n*-C<sub>8</sub>) of the crude oils were analysed on a HP5890 Gas  
303 Chromatograph (50m HP-1 column, siloxane gum used as a fixed phase) connected to an OI  
304 Analytical 4460 Sample Concentrator. A small amount of the whole crude oil was mixed with

305 deactivated alumina and transferred to the Sample Concentrator. The temperature was  
306 initially held at 30 °C for 10 minutes, then increased at a rate of 1 °C/min to 45 °C and held  
307 for 25 minutes. The eluting hydrocarbons were detected using a flame ionization detector.

308 Saturate fractions were analysed using a Varian 3700 FID gas chromatograph equipped with a  
309 30m DB-1 column. The temperature was programmed from 60 °C to 300 °C at a rate of  
310 6 °C/min and then held for 30 min at 300 °C. Gas chromatography-mass spectrometry  
311 (GCMS) was performed on a VG 7070 mass spectrometer with a gas chromatograph attached  
312 directly to the ion source (30 m (100 ft) DB-5 fused silica column used for GC separation).  
313 The temperature was initially held at 100 °C for 2 min and then programmed at 40 °C/min to  
314 180 °C and at 4 °C/min to 320 °C. After reaching 320 °C, the temperature was held for 15  
315 min. The mass spectrometer was operated with a 70 eV ionization voltage, 100 mA filament  
316 emission current, and interface temperature of 280 °C.

### 317 **3.4 Re-Os analyses**

318 The measurement of asphaltene and shale Re and Os abundances, and Re and Os isotopic  
319 compositions were undertaken at Durham University in the Laboratory for Source Rock and  
320 Sulphide Geochronology and Geochemistry (a member of the Durham Geochemistry Centre)  
321 by isotope dilution - negative thermal ionization mass spectrometry (ID-NTIMS). The  
322 chemical processing of samples to isolate and purify Re and Os and the measurement by  
323 NTIMS follow previously published protocols (Selby and Creaser, 2001; Selby and Creaser,  
324 2003; Selby, 2007; Rooney et al., 2011; Cumming et al., 2014). In brief, a known amount of

325 shale (~0.1 to 1 g) and asphaltene (~0.15 g), together with a known amount of mixed spike  
326 containing  $^{185}\text{Re}$  and  $^{190}\text{Os}$ , was digested by a  $\text{Cr}^{\text{VI}}\text{-H}_2\text{SO}_4$  solution for shale and inverse  
327 *aqua-regia* (2:1 16 N  $\text{HNO}_3$  and 12 N  $\text{HCl}$ , 9 ml) for asphaltene in carius tubes at  $220^\circ\text{C}$  for  
328 48 hrs. For some of the samples, the amount of asphaltene digested is limited by the amount  
329 of asphaltene obtained from the oil. The Os was extracted from the digested samples using  
330 chloroform, and then back-extracted from the chloroform using 9N  $\text{HBr}$ , before being  
331 purified by micro-distillation. Following the Os extraction, for shale samples, a 1 ml aliquot  
332 of the  $\text{Cr}^{\text{VI}}\text{-H}_2\text{SO}_4$  solution was evaporated to dryness, and the Re fraction was isolated using  
333 sodium hydroxide-acetone solvent extraction, before being further purified by anion  
334 chromatography. For the asphaltene samples, the *aqua-regia* was evaporated to dryness and  
335 the Re fraction purified by anion chromatography. The purified Re and Os were loaded onto  
336 Ni and Pt filaments, respectively (Selby et al., 2007). Isotopic measurements were conducted  
337 using negative thermal ionization mass spectrometry (Creaser et al., 1991; Völkening et al.,  
338 1991) on a Thermo Scientific TRITON mass spectrometer via ion-counting, using a  
339 secondary electron multiplier in peak-hopping mode for Os, and static Faraday collection for  
340 Re. In-house solution standards are  $0.1611 \pm 0.0004$  (1SD,  $n = 126$ ) for DROsS (Durham  
341 Romil Osmium Solution) and  $0.5989 \pm 0.0019$  (1SD,  $n = 116$ ) for Re Standard solution,  
342 which are in agreement with those previously reported (Luguet et al., 2008; Nowell et al.,  
343 2008; Cumming et al., 2012).

344 The measured difference in  $^{185}\text{Re}/^{187}\text{Re}$  values for the Re standard solution and the accepted  
345  $^{185}\text{Re}/^{187}\text{Re}$  value (0.5974; Gramlich et al., 1973) is used for mass fractionation correction of

346 the Re sample data. All Re and Os data are oxide and blank corrected. The total procedural  
347 blanks of inverse *aqua-regia* are  $\sim 1.6$  pg Re and  $0.04 \sim 0.1$  pg Os, with an average  
348  $^{187}\text{Os}/^{188}\text{Os}$  of  $0.24 \pm 0.06$  ( $n = 3$ ). The total procedural blanks of  $\text{Cr}^{\text{VI}}\text{-H}_2\text{SO}_4$  digested  
349 samples are  $\sim 12$  pg Re and  $0.02 \sim 0.05$  pg Os, with average  $^{187}\text{Os}/^{188}\text{Os}$  of  $0.22 \pm 0.06$  ( $n =$   
350 4). All uncertainties are determined by error propagation of uncertainties in Re and Os mass  
351 spectrometer measurements, weighing, blank abundances and isotopic compositions, spike  
352 calibrations, and the reproducibility of standard Re and Os isotopic values. The Re-Os data  
353 are regressed using *Isoplot* (V. 4.15; Ludwig, 2012) with the  $^{187}\text{Re}$  decay constant value of  
354  $1.666 \times 10^{-11} \text{ yr}^{-1}$  (Smoliar et al., 1996). This decay constant is also used for the calculation of  
355 the  $^{187}\text{Os}/^{188}\text{Os}$  values of the shales at the time of deposition and oil generation, and the  
356  $^{187}\text{Os}/^{188}\text{Os}$  values of the asphaltene at oil generation.

## 357 **4. Results**

### 358 **4.1 Asphaltene Re-Os data**

359 The asphaltene contents and Re-Os data of asphaltene fractions of this study, and one analysis  
360 reported by Selby et al. (2007), are shown in Table 3. The asphaltene abundance of the  
361 sampled Duvernay oils is between 0.23 and 14.10 %. Coupled with low asphaltene contents  
362 are low Re and Os abundances of the asphaltene fractions, which range from 0.01 to 3.78 ppb  
363 Re, 0.6 to 41.2 ppt Os, and 0.2 to 14.9 ppt  $^{192}\text{Os}$ , respectively. Oil samples possessing  
364 asphaltene abundances up to  $\sim 4$  % show a positive correlation between asphaltene abundance  
365 and both Re and  $^{192}\text{Os}$  (representing unradiogenic common Os) abundances (Fig. 4).

366 However, this relationship does not hold for the remaining oil samples that possess higher  
367 asphaltene content (6 – 8% and ~15%) (Fig. 4). Though, in general, oil samples possessing  
368 higher asphaltene contents have higher Re and  $^{192}\text{Os}$  abundances (Fig. 4). The low Re and Os  
369 abundances, coupled with the limited asphaltene obtained for Re-Os analyses, make precise  
370 measurements very challenging. The majority of the samples possess blank corrections  
371 between 0.3 – 3.3 % for Re and 1 - 10 % for Os (L02221 to L02155), although a few samples  
372 (e.g., L01810) have significant Re and Os corrections (40% Re and 50% Os). The samples  
373 with such large blank corrections also possess large uncertainties. Samples with uncertainty  
374 greater than 55% for  $^{187}\text{Re}/^{188}\text{Os}$  and 30% for  $^{187}\text{Os}/^{188}\text{Os}$  are excluded when determining a  
375 Re-Os age and are not further discussed. The  $^{187}\text{Re}/^{188}\text{Os}$  and  $^{187}\text{Os}/^{188}\text{Os}$  values of the  
376 asphaltene used for isochron construction range between ~67 and 642, and 0.78 and 1.62,  
377 respectively (Table 3). Together with the sample of Selby et al. (2007), the Re-Os data yield a  
378 Model 3 date (a model assuming variable initial  $^{187}\text{Os}/^{188}\text{Os}$  values for samples) of  $66 \pm 31$   
379 Ma ( $n = 14$ , MSWD = 6.7, initial  $^{187}\text{Os}/^{188}\text{Os} = 0.77 \pm 0.20$ ; Fig. 5-6).

#### 380 **4.2 Re-Os data for organic-rich intervals of the Duvernay Formation**

381 The Re and Os abundances and isotope data for the Duvernay source rock analysed from four  
382 wells of this study, plus those of previous studies (Selby et al., 2007; Finlay et al., 2012) are  
383 reported in Table 2. The Re and Os abundances for the Duvernay source range between 0.3  
384 and 68 ppb Re, and 29 and 1965 ppt Os. The more Re- and Os- ( $^{192}\text{Os}$ ) enriched sectors of the  
385 Duvernay source rock broadly correlate with intervals possessing higher TOC abundances

386 (Fig. 7). The  $^{187}\text{Re}/^{188}\text{Os}$  and  $^{187}\text{Os}/^{188}\text{Os}$  ratios range from ~26 to 229 and 0.49 to 1.74,  
387 respectively.

388 We have calculated the  $^{187}\text{Os}/^{188}\text{Os}$  composition of the Duvernay Formation at the time of  
389 deposition (initial  $^{187}\text{Os}/^{188}\text{Os}$  ( $\text{Os}_i$ )), a value that is equal to the  $^{187}\text{Os}/^{188}\text{Os}$  composition of  
390 the contemporaneous seawater (Cohen et al., 1999). The biostratigraphy of the Duvernay  
391 Formation shows mainly the occurrence of *Palmatolepis punctata* and *Palmatolepis hassi*  
392 (Ziegler and Sandberg, 1990; McLean and Klapper, 1998; Whalen et al., 2000), which  
393 constrains the deposition age to be between 376.5 and 380.5 Ma based on the Geologic  
394 Timescale 2016 (Ogg et al., 2016). The  $\text{Os}_i$  values for the shale samples are calculated at  
395 378.5 Ma. The  $\text{Os}_i$  values range between 0.28 and 0.38, with a Tukey's Biweight mean  
396 (which weighs the points according to their scatter from the iteratively-determined mean) of  
397  $0.33 \pm 0.01$  ( $n = 33$ ; Table 2; Fig. 7).

#### 398 **4.3 Organic geochemistry of crude oil and rock samples**

399 The Leduc-Nisku oils, although typically not altered by biodegradation or water-washing,  
400 show a wide range of thermal maturities, often resulting in variable geochemical  
401 characteristics, and have been classified into three main subgroups that include low-, normal-  
402 and high-maturity oils (Fig. 8). These hydrocarbons, however, represent a continuum that can  
403 be easily documented by examples of crude oils having maturities intermediate between the  
404 three subgroups. The following overview pertains mostly to the saturated hydrocarbon  
405 fractions of the three oil sub-types resulting from differences in thermal maturity (although

406 similar compositional variations have also been observed in the aromatic fraction by Li et al.,  
407 1998). Main compositional characteristics of the organic extracts and a brief oil-source  
408 correlation summary are also included.

409 The least mature Duvernay sourced oils are found in the Leduc and Nisku reservoirs in  
410 central eastern Alberta, to the south of the Bashaw Reef Complex. These oils are  
411 characterized by low saturate/aromatic ratio, relatively high amounts of NSO compounds,  
412 and relatively high sulphur content (1-1.5%). Gasoline range chromatograms show high *n*-  
413 heptane and methylcyclohexane peaks (*n*-C<sub>7</sub>>MCH), with toluene often in relatively high  
414 abundance compared to most other oils sourced from Devonian units. Saturate fraction gas  
415 chromatograms display smooth distribution of *n*-alkanes with slight odd carbon number  
416 preference of *n*-C<sub>15</sub> – *n*-C<sub>19</sub> members, high abundance of acyclic isoprenoids relative to *n*-  
417 alkanes, low pristane/phytane ratio (~0.80), and evident biomarkers.

418 Biomarker distributions show a smooth homohopane (C<sub>31</sub>–C<sub>35</sub>) profile, gammacerane present  
419 in moderate abundance, low amounts of rearranged hopanes (i.e. low Ts/Tm (abbreviations  
420 are annotated in Table 4)) and tricyclic and tetracyclic terpanes relative to 17 $\alpha$ (H)-hopane,  
421 C<sub>24</sub> tetracyclic terpane in similar abundance to the two C<sub>26</sub> tricyclic terpane isomers,  
422 relatively low abundances of diasteranes and short-chain steranes relative to regular steranes,  
423 and a C<sub>27</sub>-C<sub>29</sub> sterane abundance of C<sub>29</sub>>C<sub>27</sub>>>C<sub>28</sub>.

424 The majority of the oil pools along the Rimbey-Meadowbrook trend contain normal-maturity  
425 Duvernay Formation sourced oils. Compared to low maturity oils, these oils have higher

426 saturate/aromatic ratios, lower amounts of NSO compounds and lower sulphur content.

427 Gasoline range and saturate fraction gas chromatograms are generally similar in both  
428 subgroups, with notably lower abundance of acyclic isoprenoids relative to *n*-alkanes and  
429 some biomarker peaks in more mature oils.

430 Furthermore, normal maturity oils contain higher amounts of rearranged hopanes (hence  
431 higher Ts/Tm), tricyclic and tetracyclic terpanes compared to the hopanes, C<sub>24</sub> tetracyclic  
432 terpane slightly greater than C<sub>26</sub> tricyclic terpanes, very low abundance of gammacerane,  
433 higher abundances of diasteranes and short-chain steranes, and similar carbon number  
434 distributions for C<sub>27</sub>-C<sub>29</sub> regular steranes.

435 The high maturity Duvernay sourced oils and condensates tend to be those from the deeper,  
436 westerly pools with higher API gravities, typically occurring in the southern half of the  
437 province. Compared with other Duvernay sourced oils, they have higher saturate/aromatic  
438 ratios and lower amounts of NSO compounds. Although these oil can still be correlated to  
439 oils from the other two subgroups by gasoline range and saturate fraction gas  
440 chromatography data (though maturation parameters indicate higher maturity and *n*-alkane  
441 profiles shows more bias towards lower molecular weight homologues), they are quite easily  
442 distinguished based on the lack of or very low abundance of biomarkers such as hopanes and  
443 steranes. The visible peaks in the m/z 191 and m/z 217 chromatograms are typically tricyclic  
444 terpanes, Ts and C<sub>29</sub> Ts, low molecular weight steranes, high diasteranes and secosteranes  
445 with an extremely low abundance of regular steranes.

446 The analysis of the available Duvernay Formation Rock-Eval and TOC data reveals this unit  
447 contains on average 4% of organic carbon with the maximum of up to 18%, enough to be  
448 considered as petroleum source rock (Fig. 9). In thermally unaltered and low maturity  
449 samples hydrogen index values are up to 700 indicating presence of Type I-II organic matter  
450 (Fig. 10). Although the extract yields are commonly above 100 mg total extract/g TOC, and  
451 greater than 200 mg in about 1/3 of the samples, the hydrocarbon yields typically range from  
452 20 to 80, with few above 100 mg HC/g TOC (Fig. 11), which overall is indicative of good  
453 source rock potential. The extract data show no evidence of staining, as the proportions of  
454 hydrocarbons in extracts are normally less than 50% (Fig. 11)

455 The gas chromatograms of the extracts typically show *n*-alkane distributions dominated by  
456 shorter-chain homologues (*n*-C<sub>15</sub> – *n*-C<sub>20</sub>) (Fig. 12). Amounts of acyclic isoprenoids relative  
457 to *n*-alkanes are high in low maturity samples and decrease with increasing level of thermal  
458 maturity. Pristane/phytane ratios generally fall within 1-2 range. Saturate biomarker  
459 signatures of mature extracts show relatively high amounts of rearranged hopanes and  
460 steranes with no homohopane prominence, low tricyclic terpanes, Ts/Tm ratios greater than  
461 1.0 and high diasteranes. The geochemical character of the Duvernay Formation extracts is  
462 different compared with other Devonian units in Alberta that show petroleum source potential  
463 (Creaney et al., 1994).

464 Correlation of biomarker data indicates that organic geochemical composition of the  
465 thermally mature Duvernay Formation solvent extracts is very similar to that of the normal

466 maturity crude oils found within the Leduc-Nisku intervals along the Rimbey-Meadowbrook  
467 and Bashaw reef trends (Fig. 13). Both extracts and oils have higher concentrations of  $n$ -C<sub>17</sub>  
468 and  $n$ -C<sub>18</sub> relative to pristane and phytane, and average Pr/Ph ratios typical of suboxic  
469 depositional conditions (average of 1.66 and 1.38 for extracts and oils, respectively), show  
470 predominance of Ts over Tm, a smooth homohopane distributions without C<sub>34</sub> or C<sub>35</sub>  
471 prominence, relatively high amounts of rearranged steranes and common C<sub>29</sub>>C<sub>27</sub>>C<sub>28</sub>  
472 regular sterane profile (Fig. 14). Their overall similarity and genetic relationship are further  
473 supported by regional geology and stratigraphic data. As noted previously (Stoakes and  
474 Creaney, 1984 and 1985; Li et al., 1998), the Duvernay strata is the only prolific source rock  
475 interval that occurs in close stratigraphic proximity to the Leduc reefs to account for the large  
476 volume of oil found in the Leduc reservoirs and, therefore, is considered as the main source  
477 of these oils.

## 478 **5 Discussion**

### 479 **5.1 Petroleum Re-Os geochronology**

480 The burial history of the Albertan part of the Western Canada sedimentary basin has been  
481 constructed with isopach maps of the stratigraphic formations (Deroo et al., 1977; Higley et  
482 al., 2005) and basin modelling based on oil generation kinetic parameters (Higley et al., 2009;  
483 Berbesi et al., 2012), which indicate that the Duvernay Formation started to generate oil at the  
484 onset of the Laramide orogeny, i.e., around 80 Ma. According to the most recent basin models  
485 (Higley et al., 2009; Berbesi et al., 2012), the majority of the oil generation occurred between

486 ~70 and ~58 Ma, with a significant kerogen transformation ratio (>50%) of the Duvernay  
487 Formation being reached by ~65 Ma, and cessation of oil generation by ~50 Ma due to basin  
488 uplift.

489 The Re-Os oil date ( $66 \pm 31$  Ma,  $n = 14$ , MSWD = 6.7; Fig. 5) obtained from the asphaltene  
490 fraction Re-Os data, although possessing a large uncertainty, is in good agreement with the  
491 timing of peak oil generation indicated by geological modelling. It is clear that the Re-Os oil  
492 date does not in any way reflect the age of the Duvernay Formation which is the source of  
493 Duvernay oil (this study; Deroo et al., 1977; Creaney et al., 1994; Li et al., 1998), i.e. early  
494 Late Devonian (Frasnian; this study; Switzer et al., 1994).

495 The Re-Os date is derived from a Model 3 *Isoplot* solution (Ludwig, 2012), which means that  
496 the scatter about the best-fit line (the isochron), as represented by the MSWD (mean square  
497 weighted deviation) value, is due to a combination of the calculated uncertainties for the  
498  $^{187}\text{Re}/^{188}\text{Os}$  and  $^{187}\text{Os}/^{188}\text{Os}$  values and the error correlation, rho, plus an unknown but  
499 normally distributed variation in the initial  $^{187}\text{Os}/^{188}\text{Os}$  ( $\text{Os}_i$ ) values. The uncertainty in the  
500 Re-Os date spans the entire duration of oil generation; however, it is not to say that the  
501 uncertainty of the Re-Os oil age will necessarily be indicative of the duration of oil  
502 generation. The MSWD value (6.7) being >1 for the best-fit line suggests that the scatter  
503 about the best-fit line is controlled by geological factors rather than purely analytical  
504 uncertainties (Ludwig, 2012). The ~25% uncertainty in the calculated initial  $\text{Os}_i$  composition  
505 ( $0.77 \pm 0.20$ , Fig. 5; 0.55 to 1.06, Fig. 6-7, Table 3) suggests that the primary factor causing  
506 the degree of scatter about the best-fit of the Re-Os data is the variation in the  $\text{Os}_i$

507 composition of the oil sample set. The geological cause of the variation in the  $Os_i$   
508 composition of the Duvernay oil is discussed below (Section 5.2). Although the Re-Os date  
509 for the generation of Duvernay sourced oil is not as precise or detailed as the basin modeling,  
510 Re-Os oil geochronology works directly on oil samples and can provide comparison and  
511 validation of the oil generation dating by traditional geological tools in a fast and economic  
512 way.

## 513 **5.2 $^{187}Os/^{188}Os$ composition oil-source fingerprinting**

514 Previous research has proposed that at the time of oil generation, an oil inherits the  
515  $^{187}Os/^{188}Os$  composition of the source rock (Selby et al., 2005; Selby and Creaser, 2005;  
516 Finlay et al., 2011; Finlay et al., 2012; Rooney et al., 2012; Cumming et al., 2014). Compared  
517 to the previous attempts to apply the  $^{187}Os/^{188}Os$  composition of oil and source rock as an  
518 absolute fingerprinting tool, the Duvernay petroleum system benefits from its single source  
519 and simple thermal maturation history. Here we have also obtained source rock Re-Os data  
520 for the entire stratigraphic interval of the Duvernay Formation over a large geographical area,  
521 to reflect the source rock Re-Os systematics as completely as possible.

522 Although not sampled for shale geochronology, for which an intensive sampling strategy  
523 should be adopted to minimize the time span of samples and limit any possible variability in  
524 the initial  $^{187}Os/^{188}Os$  value, the Duvernay Formation source rock  $^{187}Re/^{188}Os$  and  $^{187}Os/^{188}Os$   
525 data do display a positive correlation and yield Late Devonian ages (well 10-27-57-21W4, 10  
526 samples over 55 m (180 ft), Re-Os data yield  $371 \pm 22$  Ma, initial  $^{187}Os/^{188}Os = 0.33 \pm 0.03$ ,

527 MWSD = 66; well 16-18-52-5W5, 4 samples over 1.5 m (5 ft), Re-Os data yield  $372 \pm 13$   
528 Ma, initial  $^{187}\text{Os}/^{188}\text{Os} = 0.33 \pm 0.02$ , MWSD = 0.06; well 14-29-48-6W5, 5 samples over 6  
529 m (20 ft), Re-Os data yield  $377 \pm 62$  Ma, initial  $^{187}\text{Os}/^{188}\text{Os} = 0.33 \pm 0.14$ , MWSD = 84; well  
530 2-6-47-4W5, 11 samples over 20 m (60 ft), Re-Os data yield  $360 \pm 15$  Ma, initial  $^{187}\text{Os}/^{188}\text{Os}$   
531  $= 0.38 \pm 0.03$ , MWSD = 33; Fig. 15). Further, given that the samples analysed are considered  
532 broadly the same geological age (Fig. 15A-D), we also present a calculated Re-Os date from  
533 all 33 samples. The Re-Os data for the entire sample set yield  $373.9 \pm 9.4$  Ma, with an initial  
534  $^{187}\text{Os}/^{188}\text{Os} = 0.34 \pm 0.02$  (MWSD = 82; Fig. 15E). The uncertainties of the ages are due to  
535 the variation in the  $\text{Os}_i$  compositions (Table 2, Fig. 7), which range from 0.28 to 0.38, and the  
536 limited spread in the  $^{187}\text{Re}/^{188}\text{Os}$  values ( $\leq 160$   $^{187}\text{Re}/^{188}\text{Os}$  units; Table 2 and Fig. 15).  
537 Although the Re-Os dates are imprecise, they are nominally in agreement with the Late  
538 Devonian biostratigraphic age constraints for the Duvernay Formation.

539 To evaluate the relationship between the oil  $\text{Os}_i$  (Fig. 5-6) composition and that of the source  
540 rock at the time of oil generation, the Duvernay source rock  $^{187}\text{Os}/^{188}\text{Os}$  compositions at 66  
541 Ma ( $\text{Os}_g$ ) are calculated from the present day Re-Os data of shale samples. The Duvernay  
542 Formation  $\text{Os}_g$  values range between 0.46 and 1.48 ( $n = 33$  from 7 wells), and yield a Tukey's  
543 Biweight mean of  $0.83 \pm 0.01$  (Tables 2; Fig. 7). The oil  $\text{Os}_i$  defined by the Re-Os isochron is  
544  $0.77 \pm 0.20$  (Fig. 5). The range of the individual oil  $\text{Os}_i$  values is between 0.55 and 1.06 (Fig.  
545 6). Seventy-nine percent (26 of the 33 samples) of the shale  $\text{Os}_g$  values are indistinguishable  
546 from the individual oil  $\text{Os}_i$  values (Fig. 7). The evidence from organic geochemistry of the  
547 Duvernay petroleum system indicates that the Duvernay Formation is the principal source of

548 the Duvernay oils. As such, the similarity of the oil  $Os_i$  and Duvernay Formation  $Os_g$   
549 compositions supports the research hypothesis that the oil  $Os_i$  is inherited from the source at  
550 the time of oil generation, and therefore oil  $Os_i$  and source  $Os_g$  values can be used as an oil-  
551 source correlation tool.

552 An oil-source correlation based on Os isotopic compositions is supported by the comparison  
553 of Duvernay petroleum system oil  $Os_i$  and shale  $Os_g$  values with the  $Os_g$  values of other oil-  
554 prone strata of the WCSB. As most of the oil-prone Phanerozoic strata of the WCSB  
555 underwent hydrocarbon maturation during the Laramide orogeny (Bustin, 1991; Higley et al.,  
556 2009), the  $Os_g$  values of these strata with available Re-Os data are also calculated at 66 Ma  
557 (Table 5; Fig. 16). However, in contrast to the Duvernay petroleum system oil  $Os_i$  and shale  
558  $Os_g$  values, the  $Os_g$  values of the other oil-prone strata of the WCSB are distinctly more  
559 radiogenic (e.g., the Gordondale Member of the Early Jurassic Fernie Formation (Selby et al.,  
560 2007; Finlay et al., 2012) has  $Os_g$  values are between 0.99 and 4.06, with an arithmetic  
561 average and median of 2.04 and 1.51; the Devonian-Mississippian Exshaw Formation  
562 (Creaser et al., 2002; Selby and Creaser, 2003; Finlay et al., 2012) has  $Os_g$  values between  
563 1.35 and 4.96 with an arithmetic average and median of 2.22 and 1.93; the Middle Devonian  
564 Keg River Formation (Miller, 2004) laminates of La Crete basin have  $Os_g$  values between  
565 1.34 and 4.25, with an arithmetic average and median of 1.97 and 1.64). The exceptions to  
566 the latter are the  $Os_g$  values of the kukersites of the Ordovician Yeoman Formation, Williston  
567 basin (Miller, 2004), which are between 0.46 and 5.36, with an arithmetic average and  
568 median of 1.21 and 0.84. The Ordovician kukersites  $Os_g$  values are only slightly more

569 radiogenic than the Duvernay petroleum system oil  $Os_i$  and shale  $Os_g$  values, however, it can  
570 be spatially (eastern Montana - western North Dakota and southern Saskatchewan versus  
571 south-central Alberta) excluded as the source of the Duvernay oils (Creaney et al., 1994). The  
572  $Os_i$  and  $Os_g$  data, coupled with the organic geochemistry, support the Duvernay Formation as  
573 the key source unit of the Duvernay oils, and eliminate the other oil-prone Phanerozoic strata  
574 of the WCSB as sources of the Duvernay petroleum system.

575 Although we show a strong similarity between the  $Os_i$  and  $Os_g$  values for the Duvernay oils  
576 and Formation, we observe that the  $Os_g$  values in the cores studied here and the oil  $Os_i$  values  
577 show some heterogeneity (Fig. 5-7). If we consider each core separately, the average  $Os_g$   
578 values are nominally skewed either positively or negatively to the overall average of the  $Os_g$   
579 values ( $0.83 \pm 0.01$ ; Fig. 15; Table 2). For example, the Tukey's Biweight mean of  $Os_g$  values  
580 for core 10-27-57-21W4 is  $0.72 \pm 0.12$ , for core 12-6-47-4W5 it is  $0.90 \pm 0.17$ , for core 14-  
581 29-48-6W5 it is  $0.96 \pm 0.07$ , and for core 16-18-52-5W5 the arithmetic average is  $0.66 \pm 0.22$   
582 (2 SD; weighted by assigned errors only as Tukey's Biweight mean is not suitable for its  
583 small sample set).

584 The change in the  $^{187}Os/^{188}Os$  composition from the time of source rock deposition to the  
585 time of oil generation is dependent on the duration between deposition and hydrocarbon  
586 maturation, and the Re abundance in the source rock. Variability in the Re abundance  
587 stratigraphically, plus the variations in local seawater  $^{187}Os/^{188}Os$  values inherited by the  
588 organic-rich rock, such as that shown by the Duvernay Formation (Table 2), results in  
589 heterogeneous  $^{187}Os/^{188}Os$  values with  $^{187}Re$  decay (Table 2; Fig. 7 and 15).

590 As such, if the heterogeneous  $Os_g$  is inherited by the generated oils then our data propose that  
591 the oil generated from different geographical sections of the same source interval could lead  
592 to reservoir oils possessing variable  $Os_i$ . The primary migration and expulsion of oil within  
593 and from a source rock, which is often broadly contemporaneous with or occurs shortly after  
594 oil generation, could result in the homogenization of the  $^{187}Os/^{188}Os$  values of oil. Although,  
595 the extent of homogenization should depend on many factors (e.g. permeability of source  
596 rock and carrier beds). In the case of the Duvernay Formation, the oils generated could  
597 possess a range in  $Os_i$  from 0.46 to 1.48, which is similar to what is observed in this study  
598 with the Duvernay oil  $Os_i$  values, ranging from  $\sim 0.55$  to 1.06 (Table 2 - 3; Fig. 5-7). The  
599 variability in the  $Os_i$  values makes it analytically challenging to obtain a precise isochron ( $66$   
600  $\pm 31$  Ma). The determined  $Os_i$  by the isochron ( $0.77 \pm 0.20$ ) demonstrates the variability in  
601 the  $Os_i$  values. As such, if we select the samples with the most similar  $Os_i$  (e.g., L00864,  
602 L00873, L02196, L02220 and L02221), a Re-Os date of  $56 \pm 18$  Ma is obtained, with an  $Os_i$   
603 of  $0.74 \pm 0.10$  and MSWD of 0.33. The Re-Os date still coincides with the timing of  
604 hydrocarbon maturation associated with the Laramide orogeny, but is almost 50% more  
605 precise.

### 606 **5.3 Oil Re-Os systematics: effect of oil-water contact**

607 Although we propose that the Re and Os in oil are inherited from a source rock, based on the  
608 similarity of the  $Os_i$  values of the asphaltene fractions and the  $Os_g$  values of the Duvernay  
609 Formation shales, an experimental study has suggested that Re and Os in oil can also be  
610 derived from contact with formation water (Mahdaoui et al., 2015). The outcome of this

611 experimental work has recently been questioned (Wu et al., 2016), particularly based on the  
612 several orders of magnitude higher Re and Os concentrations applied in the experiment  
613 (0.001 to 100  $\mu\text{g/g}$  Re and 1 or 10  $\text{ng/g}$  Os) compared with the known low Re and Os  
614 concentrations of basin fluids (typically 4  $\text{pg/g}$  Re and 70  $\text{fg/g}$  Os; Mahdaoui et al. (2015)) in  
615 most oil-bearing sedimentary basins. Nevertheless, we consider here if the oil Re-Os  
616 systematics may have been affected by or originated from the basin fluids in the Leduc reef  
617 trend and Nisku Formation. There are very limited Re and Os data for basin fluids available  
618 at present and if we also use the typical formation water Re and Os abundances of 4  $\text{pg/g}$  and  
619 70  $\text{fg/g}$ , respectively (Mahdaoui et al., 2015), approximately 2 to 40 g of such water contains  
620 equivalent Re and Os in 1 gram of Duvernay oil (Table 3). Such oil-water contact ratios are  
621 highly probable in a petroleum system (Magoon and Dow, 1991). As such, based on the  
622 experiments of Mahdaoui et al. (2015), the Re-Os systematics of the low Re- and Os-bearing  
623 Duvernay oils could have been easily influenced by oil-basin fluid interaction and reflect the  
624 Os isotopic composition of the basin fluid. However, comparing the  $^{87}\text{Sr}/^{86}\text{Sr}$  values of Late  
625 Devonian seawater of 0.7080 - 0.7084 (Burke et al., 1982) with the  $^{87}\text{Sr}/^{86}\text{Sr}$  values of  
626 calcites and dolomite cements (0.7088 - 0.7108) of the Leduc Rimbey-Meadowbrook reef  
627 trend (Stasiuk, 1997), and that of the current brines of Nisku Formation (0.70998-0.71206)  
628 and Leduc Formation (0.70872 - 0.70981) (Connolly et al., 1990), it is suggested that the  
629 basin fluids could have interacted with the radiogenic crystalline basement and/or Proterozoic  
630 - Lower Cambrian clastics (Mountjoy et al., 1999). As such, the  $^{187}\text{Os}/^{188}\text{Os}$  compositions of  
631 the basin fluids should be radiogenic, considering the high  $^{187}\text{Os}/^{188}\text{Os}$  initial values of these

632 strata (Kendall et al., 2009) and the long duration between the depositional age and the timing  
633 of oil generation. For example, the Neoproterozoic Old Fort Point Formation has an initial  
634  $^{187}\text{Os}/^{188}\text{Os}$  value of  $\sim 0.62$  at deposition of 608 Ma (Kendall et al., 2004), which will have  
635 radiogenically evolved to  $^{187}\text{Os}/^{188}\text{Os}$  values  $>3$  at 66 Ma (Table 5). Further, considering a  
636 lower end member  $^{187}\text{Re}/^{188}\text{Os}$  value of 100 for the crystalline basement and/or Proterozoic -  
637 Lower Cambrian strata and an initial  $^{187}\text{Os}/^{188}\text{Os}$  composition of 0.5, the decay of  $^{187}\text{Re}$  over  
638  $\geq 450$  million years will yield a  $^{187}\text{Os}/^{188}\text{Os}$  value  $> 1.25$  at the time that the Duvernay  
639 Formation underwent thermal maturation. The deep-originated basinal fluids interacted with  
640 old strata and therefore should have very radiogenic  $^{187}\text{Os}/^{188}\text{Os}$  compositions. The minimum  
641 estimate of the  $^{187}\text{Os}/^{188}\text{Os}$  composition of the basinal fluid is more radiogenic than the  
642 present day (0.78 – 1.62) and initial ( $0.77 \pm 0.20$ ) values of the Duvernay oil . As a result, we  
643 propose that the predominant Re and Os budget and the isotope systematics of the Duvernay  
644 oil represent that inherited from the Duvernay Formation source rocks during thermal  
645 maturation, and not Re and Os sequestered from basin fluids. And therefore the  $\text{Os}_i$  values are  
646 inherited at the time of oil generation, and are ultimately linked to the source rock rather than  
647 formation fluids.

## 648 **Conclusions**

649 Despite the uncertainty of Re-Os asphaltene isotopic data of the Duvernay oils, which is a  
650 direct result of the low Re and Os abundance, the limited range in the  $^{187}\text{Re}/^{188}\text{Os}$  values, and  
651 the variation in the  $\text{Os}_i$  values of the asphaltene, the Re-Os age derived from asphaltene

652 fractions agrees well with the widely accepted burial and hydrocarbon maturation models that  
653 indicate that hydrocarbon generation occurred long after source rock deposition during the  
654 Laramide orogeny. Further, the similarity between the oil  $Os_i$  values and the Duvernay  
655 Formation  $Os_g$  values, and their difference to other oil-prone strata of the WCSB, coupled  
656 with the evidence from organic geochemistry, confirms the Duvernay Formation as the  
657 source and the ability of the  $^{187}Os/^{188}Os$  composition as an oil-source correlation tool.  
658 Moreover, the Duvernay-sourced oils Re-Os systematics are not considered to have been  
659 significantly affected by basin fluids, indicating that the majority of Re-Os systematics in the  
660 oil (asphaltene fraction) is inherited from its source.

661 We suggest that one of the major factors controlling the precision of a Re-Os date for oil  
662 relates to the variation in  $Os_i$  values inherited by an oil from its source at the time of oil  
663 generation, which is independent of the radiogenic evolution of the  $^{187}Os/^{188}Os$  composition  
664 in the source rock. For example, the relative homogeneous  $^{187}Os/^{188}Os$  of Duvernay  
665 Formation at the time of deposition ( $Os_i = \sim 0.33$ ) evolved with time to a heterogeneous  
666  $^{187}Os/^{188}Os$  composition due to the variable Re abundance in the source unit. The  
667 heterogeneous  $^{187}Os/^{188}Os$  composition of the Duvernay Formation was inherited by the  
668 generated oil. Our data suggests that basin wide thorough homogenization of the Os isotopic  
669 composition did not occur during migration.

670 The agreement of the Re-Os asphaltene date, coupled with the similarity of the  $Os_i$  and  $Os_g$   
671 values of the asphaltene and Duvernay Formation, respectively, of the relatively simple

672 Duvernay petroleum system of Western Canada sedimentary basin with basin models and  
673 organic geochemistry confirms the potential ability of the Re-Os oil (asphaltene fraction)  
674 systematics to record the timing of hydrocarbon generation, and to serve as an effective oil-  
675 source correlation tool.

676

677 **References**

- 678 Adams, J., S. Larter, B. Bennett, H. Huang, J. Westrich, and C. van Kruisdijk, 2013, The  
679 dynamic interplay of oil mixing, charge timing, and biodegradation in forming the  
680 Alberta oil sands: Insights from geologic modeling and biogeochemistry, *in* F. J. Hein,  
681 D. Leckie, S. Larter, and J. R. Suter, eds., Heavy-oil and oil-sand petroleum systems  
682 in Alberta and beyond: AAPG Studies in Geology 64, p. 23–102.  
683 DOI:10.1306/13371578St643552.
- 684 Aitken, J.D., and D. K. Norris, 2014, WEBLEX Canada, Lexicon of Canadian geologic  
685 names on-line, <[http://weblex.nrcan.gc.ca/weblexnet4/weblex\\_e.aspx](http://weblex.nrcan.gc.ca/weblexnet4/weblex_e.aspx)>, accessed  
686 November 2017.
- 687 Amthor, J. E., E. W. Mountjoy, and H. G. Machel, 1994, Regional-scale porosity and  
688 permeability variations in Upper Devonian Leduc buildups: Implications for reservoir  
689 development and prediction in carbonates: AAPG Bulletin, v. 78, no. 10, p. 1541-  
690 1558. doi:10.1306/a25ff215-171b-11d7-8645000102c1865d
- 691 Anders, D. E., J. G. Palacas, and R. C. Johnson, 1992, Thermal maturity of rocks and 944  
692 hydrocarbon deposits, Uinta Basin, Utah, *in* Thomas D. Fouch, Vito F. Nuccio,  
693 Thomas C. Chidsey, Jr., eds., Hydrocarbon and mineral resources of the Uinta Basin,  
694 Utah and Colorado: Utah Geological Association Guidebook, no. 20, p. 53-74.
- 695 Behar, F., V. Beaumont, H. L. Penteadó, and B. De, 2001, Rock-Eval 6 Technology:  
696 Performances and developments. Revue de l' Français du Pétrole, v. 56, no. 2, p. 111-  
697 134. DOI: 10.2516/ogst:2001013

698 Berbesi, L. A., R. di Primio, Z. Anka, B. Horsfield, and D. K. Higley, 2012, Source rock  
699 contributions to the Lower Cretaceous heavy oil accumulations in Alberta: A basin  
700 modeling study: AAPG Bulletin, v. 96, no. 7, p. 1211-1234. DOI:  
701 10.1306/11141111064

702 Burke, W., R. Denison, E. Hetherington, R. Koepnick, H. Nelson, and J. Otto, 1982,  
703 Variation of seawater  $^{87}\text{Sr}/^{86}\text{Sr}$  throughout Phanerozoic time: Geology, v. 10, no. 10, p.  
704 516-519. DOI: 10.1130/0091-7613(1982)10<516:VOSSTP>2.0.CO;2

705 Bustin, R., 1991, Organic maturity in the Western Canada sedimentary basin: International  
706 Journal of Coal Geology, v. 19, no. 1, p. 319-358. DOI: 10.1016/0166-  
707 5162(91)90026-F

708 Chow, N., J. Wendte, and L. D. Stasiuk, 1995, Productivity versus preservation controls on  
709 two organic-rich carbonate facies in the Devonian of Alberta: Sedimentological and  
710 organic petrological evidence: Bulletin of Canadian Petroleum Geology, v. 43, no. 4,  
711 p. 433-460.

712 Cohen, A. S., A. L. Coe, J. M. Bartlett, and C. J. Hawkesworth, 1999, Precise Re–Os ages of  
713 organic-rich mudrocks and the Os isotope composition of Jurassic seawater: Earth and  
714 Planetary Science Letters, v. 167, no. 3-4, p. 159-173. DOI: 10.1016/s0012-  
715 821x(99)00026-6

716 Connolly, C. A., L. M. Walter, H. Baadsgaard, and F. J. Longstaffe, 1990, Origin and  
717 evolution of formation waters, Alberta basin, Western Canada sedimentary basin. II.  
718 Isotope systematics and water mixing: Applied Geochemistry, v. 5, no. 4, p. 397-413.

719 DOI: 10.1016/0883-2927(90)90017-Y

720 Creaney, S., and J. Allan, 1990, Hydrocarbon generation and migration in the Western  
721 Canada sedimentary basin: Geological Society, London, Special Publications, v. 50,  
722 no. 1, p. 189-202. DOI: 10.1144/GSL.SP.1990.050.01.9

723 Creaney, S., 1992, Petroleum Systems in the foreland basin of Western Canada, *in* R.  
724 Macqueen and D. Leckie, eds., Foreland basins and fold belts: AAPG Memoir 55, p.  
725 279-308.

726 Creaney, S., J. Allan, K. Cole, M. Fowler, P. Brooks, K. Osadetz, R. Macqueen, L. Snowdon,  
727 and C. Riediger, 1994, Petroleum generation and migration in the Western Canada  
728 sedimentary basin, *in* G. D. Mossop and I. Shetson, eds., Geological Atlas of the  
729 Western Canada sedimentary basin, p. 455-468.

730 Creaser, R. A., P. Sannigrahi, T. Chacko, and D. Selby, 2002, Further evaluation of the Re-Os  
731 geochronometer in organic-rich sedimentary rocks: A test of hydrocarbon maturation  
732 effects in the Exshaw Formation, Western Canada sedimentary basin: *Geochimica et*  
733 *Cosmochimica Acta*, v. 66, no. 19, p. 3441-3452. DOI: 10.1016/S0016-  
734 7037(02)00939-0

735 Cumming, V. M., D. Selby, and P. G. Lillis, 2012, Re–Os geochronology of the lacustrine  
736 Green River Formation: Insights into direct depositional dating of lacustrine  
737 successions, Re–Os systematics and paleocontinental weathering: *Earth and Planetary*  
738 *Science Letters*, v. 359-360, p. 194-205. DOI: 10.1016/j.epsl.2012.10.012

739 Cumming, V. M., D. Selby, P. G. Lillis, and M. D. Lewan, 2014, Re–Os geochronology and

740 Os isotope fingerprinting of petroleum sourced from a Type I lacustrine kerogen:  
741 Insights from the natural Green River petroleum system in the Uinta basin and  
742 hydrous pyrolysis experiments: *Geochimica et Cosmochimica Acta*, v. 138, p. 32-56.  
743 DOI: 10.1016/j.gca.2014.04.016

744 Deroo, G., T. G. Powell, B. Tissot, and R. G. McCrossan, 1977, The origin and migration of  
745 petroleum in the Western Canadian sedimentary basin, Alberta - A geochemical and  
746 thermal maturation study: *Geological Survey of Canada Bulletin* 262, 136 p.

747 Dunn, L., G. Schmidt, K. Hammermaster, M. Brown, R. Bernard, E. Wen, R. Befus, and S.  
748 Gardiner, 2012, The Duvernay Formation (Devonian): Sedimentology and reservoir  
749 characterization of a shale gas/liquids play in Alberta, Canada (abs.), *in* *Proceedings*  
750 *Canadian Society of Petroleum Geologists: Annual Convention, Calgary.*

751 Eadington, P., P. Hamilton, and G. Bai, 1991, Fluid history analysis - A new concept for  
752 prospect evaluation: *Australian Petroleum Exploration Association Journal*, v. 31, no.  
753 1, p. 282-294.

754 Energy Resources Conservation Board, Calgary, Alberta, Canada, 2009, Table of  
755 formations, Alberta, <[ags.aer.ca/document/Table-of-Formations.pdf](http://ags.aer.ca/document/Table-of-Formations.pdf)>, accessed  
756 December 12, 2014.

757 English, J. M. and S. T. Johnston, 2004, The Laramide orogeny: what were the driving  
758 forces?. *International Geology Review*, v. 46, no. 9, p. 833-838. DOI: 10.2747/0020-  
759 6814.46.9.833.

760 Espitalie, J., G. Deroo, and F. Marquis, 1985, *Rock Eval Pyrolysis and Its Applications.*

761 Preprint; Institut Francais du Petrole, Geologie No. 27299, 72 p. English translation  
762 of, La pyrolyse Rock-Eval et ses applications, Premiere, Deuxieme et Troisieme  
763 Parties, in Revue de l'Institut Francais du Petrole, v. 40, p. 563-579 and 755-784; v.  
764 41, p. 73-89. DOI: 10.2516/ogst:1985035

765 Evans, C. R., M. A. Rogers, and N. J. L. Bailey, 1971, Evolution and alteration of petroleum  
766 in Western Canada: *Chemical Geology*, v. 8, no. 3, p. 147-170.

767 Finlay, A. J., D. Selby, M. J. Osborne, and D. Finucane, 2010, Fault-charged mantle-fluid  
768 contamination of United Kingdom North Sea oils: Insights from Re-Os isotopes:  
769 *Geology*, v. 38, no. 11, p. 979-982. DOI: 10.1130/G31201.1

770 Finlay, A. J., D. Selby, and M. J. Osborne, 2011, Re-Os geochronology and fingerprinting of  
771 United Kingdom Atlantic Margin oil: Temporal implications for regional petroleum  
772 systems: *Geology*, v. 39, no. 5, p. 475-478. DOI: 10.1130/G31781.1

773 Finlay, A. J., D. Selby, and M. J. Osborne, 2012, Petroleum source rock identification of  
774 United Kingdom Atlantic Margin oil fields and the Western Canadian Oil Sands using  
775 Platinum, Palladium, Osmium and Rhenium: Implications for global petroleum  
776 systems: *Earth and Planetary Science Letters*, v. 313-314, p. 95-104. DOI:  
777 10.1016/j.epsl.2011.11.003

778 Fothergill, P. A., D. Boskovic, P. Murphy, M. Mukati, and N. Schoellkopf, 2014, Regional  
779 Modelling of the Late Devonian Duvernay Formation, Western Alberta, Canada:  
780 *Unconventional Resources Technology Conference (URTEC)*, p. 95-102..

781 Fowler, M. G., L. D. Stasiuk, M. Hearn, and M. Obermajer, 2001, Devonian hydrocarbon

782 source rocks and their derived oils in the Western Canada sedimentary basin: Bulletin  
783 of Canadian Petroleum Geology, v. 49, no. 1, p. 117-148. DOI: 10.2113/49.1.117

784 Fowler, M. G., M. Obermajer, and L. D. Stasiuk, 2003, Rock-Eval/TOC data for Devonian  
785 potential source rocks, Western Canada sedimentary basin: Geological Survey of  
786 Canada Open File 1579. DOI: dx.doi.org/10.4095/214440

787 Ge, X., C. Shen, D. Selby, D. Deng, and L. Mei, 2016, Apatite fission-track and Re-Os  
788 geochronology of the Xuefeng uplift, China: Temporal implications for dry gas  
789 associated hydrocarbon systems: *Geology*, v. 44, no. 6, p. 491-494. DOI:  
790 10.1130/G37666.1

791 Ge, X., C. Shen, D. Selby, J. Wang, L. Ma, X. Ruan, S. Hu, L. Mei, 2017, Petroleum  
792 generation timing and source in the Northern Longmen Shan Thrust Belt, Southwest  
793 China: Implications for multiple oil generation episodes and sources: *AAPG Bulletin*,  
794 in press. DOI: 10.1306/07111716230 17125

795 Georgiev, S. V., H. J. Stein, J. L. Hannah, R. Galimberti, M. Nali, G. Yang, and A.  
796 Zimmerman, 2016, Re-Os dating of maltenes and asphaltenes within single samples  
797 of crude oil: *Geochimica et Cosmochimica Acta*, v. 179, p. 53-75. DOI:  
798 10.1016/j.gca.2016.01.016

799 Gramlich, J. W., T. J. Murphy, E. L. Garner, and W. R. Shields, 1973, Absolute isotopic  
800 abundance ratio and atomic weight of a reference sample of rhenium: *Journal of*  
801 *Research of the National Bureau of Standards – A. Physics and Chemistry*, v. 77A, no.  
802 6, p. 691–698. DOI: 10.6028/jres.077A.040

803 Harris, S. A., M. J. Whiticar, and M. G. Fowler, 2003, Classification of Duvernay sourced  
804 oils from central and southern Alberta using Compound Specific Isotope Correlation  
805 (CSIC): Bulletin of Canadian Petroleum Geology, v. 51, no. 2, p. 99-125. DOI:  
806 10.2113/51.2.99

807 Higley, D. K., M. Henry, L. N. R. Roberts, and D. W. Steinshouer, 2005, 1-D/3-D geologic  
808 model of the Western Canada sedimentary basin: The Mountain Geologist, v. 42, no.  
809 2, p. 53-66.

810 Higley, D. K., M. D. Lewan, L. N. R. Roberts, and M. Henry, 2009, Timing and petroleum  
811 sources for the Lower Cretaceous Mannville Group oil sands of northern Alberta  
812 based on 4-D modeling: AAPG Bulletin, v. 93, no. 2, p. 203-230. DOI:  
813 10.1306/09150808060

814 Issler, D. R., S. D. Willett, C. Beaumont, R. A. Donelick, and A. M. Grist, 1999,  
815 Paleotemperature history of two transects across the Western Canada sedimentary  
816 basin: Constraints from apatite fission track analysis: Bulletin of Canadian Petroleum  
817 Geology, v. 47, no. 4, p. 475-486.

818 Jenden, P. D., and F. Monnier, 1997, Regional variations in initial petroleum potential of the  
819 Upper Devonian Duvernay and Muskwa formations, Central Alberta (abs.): Canadian  
820 Society of Petroleum Geologists - SEPM Joint Convention: Program with Abstracts,  
821 Calgary, p. 146

822 Kelley, S., 2002, K-Ar and Ar-Ar dating: Reviews in Mineralogy and Geochemistry, v. 47,  
823 no. 1, p. 785-818. DOI: 10.2138/rmg.2002.47.17

824 Kendall, B. S., R. A. Creaser, G. M. Ross, and D. Selby, 2004, Constraints on the timing of  
825 Marinoan “Snowball Earth” glaciation by  $^{187}\text{Re}$ - $^{187}\text{Os}$  dating of a Neoproterozoic,  
826 post-glacial black shale in Western Canada: *Earth and Planetary Science Letters*, v.  
827 222, no. 3-4, p. 729-740. DOI: 10.1016/j.epsl.2004.04.004

828 Kendall, B., R. A. Creaser, and D. Selby, 2009,  $^{187}\text{Re}$ - $^{187}\text{Os}$  geochronology of Precambrian  
829 organic-rich sedimentary rocks: Geological Society, London, Special Publications, v.  
830 326, no. 1, p. 85-107. DOI: 10.1144/SP326.5

831 Lamers, E., and S. M. M. Carmichael, 1999, The Paleocene deepwater sandstone play West  
832 of Shetland: Geological Society of London, Petroleum Geology Conference series, v.  
833 5, p. 645-659. DOI: 10.1144/0050645

834 Li, M., H. Yao, M. G. Fowler, and L. D. Stasiuk, 1998, Geochemical constraints on models  
835 for secondary petroleum migration along the Upper Devonian Rimbey-Meadowbrook  
836 reef trend in central Alberta, Canada: *Organic Geochemistry*, v. 29, no. 1-3, p. 163-  
837 182. DOI: 10.1016/s0146-6380(98)00094-1

838 Lillis, P. G., and D. Selby, 2013, Evaluation of the rhenium–osmium geochronometer in the  
839 Phosphoria petroleum system, Bighorn basin of Wyoming and Montana, USA:  
840 *Geochimica et Cosmochimica Acta*, v. 118, p. 312-330. DOI:  
841 10.1016/j.gca.2013.04.021

842 Ludwig, K., 2012, User’s manual for Isoplot version 3.75-4.15: a geochronological toolkit for  
843 Microsoft: Excel Berkley Geochronological Center Special Publication, no. 5.

844 Luguet, A., G. M. Nowell and D. G. Pearson, 2008,  $^{184}\text{Os}/^{188}\text{Os}$  and  $^{186}\text{Os}/^{188}\text{Os}$

845 measurements by negative thermal ionisation mass spectrometry (N-TIMS): Effects  
846 of interfering element and mass fractionation corrections on data accuracy and  
847 precision. *Chemical Geology*, v. 248, no. 3, p. 342–362. DOI:  
848 10.1016/j.chemgeo.2007.10.013

849 Magoon, L., and W. Dow, 1991, The petroleum system - From source to trap: AAPG  
850 Bulletin, v. 75, no.3, p. 627.

851 Mahdaoui, F., R. Michels, L. Reisberg, M. Pujol, and Y. Poirier, 2015, Behavior of Re and Os  
852 during contact between an aqueous solution and oil: Consequences for the application  
853 of the Re–Os geochronometer to petroleum: *Geochimica et Cosmochimica Acta*, v.  
854 158, p. 1-21. DOI: 10.1016/j.gca.2015.02.009

855 Mark, D. F., J. Parnell, S. P. Kelley, M. Lee, S. C. Sherlock, and A. Carr, 2005, Dating of  
856 multistage fluid flow in sandstones: *Science*, v. 309, no. 5743, p. 2048-2051. DOI:  
857 10.1126/science.1116034

858 Mark, D. F., J. Parnell, S. P. Kelley, M. R. Lee, and S. C. Sherlock, 2010,  $^{40}\text{Ar}/^{39}\text{Ar}$  dating of  
859 oil generation and migration at complex continental margins: *Geology*, v. 38, no. 1, p.  
860 75-78. DOI: 10.1130/G30237.1

861 Marquez, X., 1994, Reservoir geology of Upper Devonian Leduc buildups, deep Alberta  
862 basin: Ph. D. Dissertation, McGill University, Montreal, Canada, 285 p.

863 McLean, R. A., and G. Klapper, 1998, Biostratigraphy of Frasnian (Upper Devonian) strata in  
864 western Canada, based on conodonts and rugose corals: *Bulletin of Canadian*  
865 *Petroleum Geology*, v. 46, no. 4, p. 515-563.

866 Miller, C. A., 2004, Re-Os dating of algal laminites reduction-enrichment of metals in the  
867 sedimentary environment and evidence for new geoporphyryns: Master of Science  
868 Dissertation, University of Saskatchewan, Saskatoon, Canada, 153 p. DOI:  
869 handle:10388/etd-06242011-085331

870 Mountjoy, E. W., H. G. Machel, D. Green, J. Duggan, and A. E. Williams-Jones, 1999,  
871 Devonian matrix dolomites and deep burial carbonate cements: a comparison between  
872 the Rimbey-Meadowbrook reef trend and the deep basin of west-central Alberta:  
873 Bulletin of Canadian Petroleum Geology, v. 47, no. 4, p. 487-509.

874 Nowell, G., A. Luguet, D. Pearson, and M. Horstwood, 2008, Precise and accurate  
875  $^{186}\text{Os}/^{188}\text{Os}$  and  $^{187}\text{Os}/^{188}\text{Os}$  measurements by multi-collector plasma ionisation mass  
876 spectrometry (MC-ICP-MS) part I: Solution analyses: Chemical Geology, v. 248, no.  
877 3, p. 363-393. DOI: 10.1016/j.chemgeo.2007.10.020

878 Ogg, J., G. Ogg, and F. M. Gradstein, 2016, A Concise Geologic Time Scale 2016,  
879 Amsterdam, Elsevier, 242 p.

880 Peters, K. E., C. C. Walters, and J. M. Moldowan, 2005, The biomarker guide, volume 2 -  
881 Biomarkers and isotopes in petroleum exploration and earth history: Cambridge:  
882 Cambridge University Press, v. 475, 634 p.

883 Powell, T.G., 1978, An assessment of the hydrocarbon source rock potential of the Canadian  
884 Arctic Islands. Geological Survey of Canada, Paper 78-12, 82 p.

885 Riediger, C. L., S. Ness, M. Fowler, and N. T. Akpulat, 2001, Timing of oil generation and  
886 migration, northeastern British Columbia and southern Alberta - Significance for

887 understanding the development of the eastern Alberta tar sands deposits (abs.): AAPG  
888 Annual Convention Official Program, v. 10, p. A168.

889 Rogers, M. A., J. McAlary, and N. Bailey, 1974, Significance of reservoir bitumens to  
890 thermal-maturation studies, Western Canada basin: AAPG Bulletin, v. 58, no. 9, p.  
891 1806-1824.

892 Rooney, A. D., D. M. Chew, and D. Selby, 2011, Re–Os geochronology of the  
893 Neoproterozoic–Cambrian Dalradian Supergroup of Scotland and Ireland:  
894 Implications for Neoproterozoic stratigraphy, glaciations and Re–Os systematics:  
895 Precambrian Research, v. 185, no. 3-4, p. 202-214. DOI:  
896 10.1016/j.precamres.2011.01.009

897 Rooney, A. D., D. Selby, M. D. Lewan, P. G. Lillis, and J. P. Houzay, 2012, Evaluating Re–  
898 Os systematics in organic-rich sedimentary rocks in response to petroleum generation  
899 using hydrous pyrolysis experiments: *Geochimica et Cosmochimica Acta*, v. 77, p.  
900 275-291. DOI: 10.1016/j.gca.2011.11.006

901 Rostron, B. J., 1997, Fluid flow, hydrochemistry and petroleum entrapment in Devonian reef  
902 complexes, south-central Alberta, Canada. *in* S.G. Pemberton and D.P. James eds.,  
903 Petroleum Geology of the Cretaceous Mannville Group: Canadian Society of  
904 Petroleum Geologists Memoir 18, Calgary, p. 169-190.

905 Ruble, T. E., M. Lewan, and R. Philp, 2001, New insights on the Green River petroleum  
906 system in the Uinta basin from hydrous pyrolysis experiments: AAPG bulletin, v. 85,  
907 no. 8, p. 1333-1371.

908 Selby, D., and R. A. Creaser, 2001, Re-Os geochronology and systematics in molybdenite  
909 from the Endako porphyry molybdenum deposit, British Columbia, Canada:  
910 *Economic Geology*, v. 96, no. 1, p. 197-204. DOI: 10.2113/gsecongeo.96.1.197

911 Selby, D., and R. A. Creaser, 2003, Re-Os geochronology of organic rich sediments: an  
912 evaluation of organic matter analysis methods: *Chemical Geology*, v. 200, no. 3-4, p.  
913 225-240. DOI: 10.1016/s0009-2541(03)00199-2

914 Selby, D., and R. A. Creaser, 2005a, Direct radiometric dating of hydrocarbon deposits using  
915 rhenium-osmium isotopes: *Science*, v. 308, no. 5726, p. 1293-1295. DOI:  
916 10.1126/science.1111081

917 Selby, D., and R. A. Creaser, 2005b, Direct radiometric dating of the Devonian-Mississippian  
918 time-scale boundary using the Re-Os black shale geochronometer: *Geology*, v. 33, no.  
919 7, p. 545-548. DOI: 10.1130/g21324.1

920 Selby, D., R. Creaser, K. Dewing, and M. Fowler, 2005, Evaluation of bitumen as a Re-Os  
921 geochronometer for hydrocarbon maturation and migration: A test case from the  
922 Polaris MVT deposit, Canada: *Earth and Planetary Science Letters*, v. 235, no. 1-2, p.  
923 1-15. DOI: 10.1016/j.epsl.2005.02.018

924 Selby, D., 2007, Direct Rhenium-Osmium age of the Oxfordian-Kimmeridgian boundary,  
925 Staffin bay, Isle of Skye, UK, and the Late Jurassic time scale: *Norwegian Journal of*  
926 *Geology*, v. 87, no. 3, p. 291-299.

927 Selby, D., R. A. Creaser, and M. G. Fowler, 2007, Re-Os elemental and isotopic systematics  
928 in crude oils: *Geochimica et Cosmochimica Acta*, v. 71, no. 2, p. 378-386. DOI:

929 10.1016/j.gca.2006.09.005

930 Simpson, G. P., 1999, Sulfate reduction and fluid chemistry of the Devonian Leduc and Nisku  
931 formations in south-central Alberta: Ph. D. Dissertation, University of Calgary,  
932 Canada, 228 p.

933 Smoliar, M. I., R. J. Walker, and J. W. Morgan, 1996, Re-Os ages of group IIA, IIIA, IVA,  
934 and IVB iron meteorites: *Science*, v. 271, no. 5252, p. 1099.

935 Speight, J., 2004, Petroleum Asphaltenes-Part 1: Asphaltenes, resins and the structure of  
936 petroleum: *Oil & Gas Science and Technology*, v. 59, no. 5, p. 467-477. DOI:  
937 10.2516/ogst:2004032

938 Stasiuk, L. D., 1997, The origin of pyrobitumens in upper Devonian Leduc formation gas  
939 reservoirs, Alberta, Canada: An optical and EDS study of oil to gas transformation:  
940 *Marine and Petroleum Geology*, v. 14, no. 7-8, p. 915-929. DOI: 10.1016/S0264-  
941 8172(97)00031-7

942 Stasiuk, L. D., and M. Fowler, 2002, Thermal maturity evaluation (vitrinite and vitrinite  
943 reflectance equivalent) of Middle Devonian, Upper Devonian and Devonian-  
944 Mississippian strata in the Western Canada Sedimentary basin: Geological Survey of  
945 Canada Open File Report 4341, 20 p. DOI: 10.4095/213610

946 Stoakes, F., and S. Creaney, 1984, Sedimentology of a carbonate source rock: the Duvernay  
947 Formation of Central Alberta, *in* L. Eliuk, eds., *Carbonates in subsurface and outcrop:*  
948 *Canadian Society of Petroleum Geologists Core Conference*, p. 132-147.

949 Stoakes, F., and S. Creaney, 1985, Controls on the accumulation and subsequent maturation

950 and migration history of a carbonate source rock. Society of Economic  
951 Paleontologists and Mineralogists, *in* Proceedings SEPM Core Workshop  
952 Proceedings, Golden, Colorado, p. 343-375.

953 Switzer, S., W. Holland, D. Christie, G. Graf, A. Hedinger, R. McAuley, R. Wierzbicki, and J.  
954 Packard, 1994, Devonian Woodbend-Winterburn strata of the Western Canada  
955 sedimentary basin: Geological Atlas of the Western Canada sedimentary basin:  
956 Canadian Society of Petroleum Geologists and Alberta Research Council, p. 165-202.

957 Tozer, R. S., A. P. Choi, J. T. Pietras, and D. J. Tanasichuk, 2014, Athabasca oil sands:  
958 Megatrap restoration and charge timing: AAPG Bulletin, v. 98, no. 3, p. 429-447.  
959 DOI: 10.1306%2F08071313039

960 Völkening, J., T. Walczyk, and K.G. Heumann, 1991, Osmium isotope ratio determination by  
961 negative thermal ion mass spectrometry: International Journal of Mass Spectrometry  
962 and Ion Processes, v. 105, no. 2, p. 147–159. DOI: 10.1016/0168-1176(91)80077-Z

963 Welte, D. H., B. Horsfield, and D. R. Baker, 2012, Petroleum and basin evolution: insights  
964 from petroleum geochemistry, geology and basin modeling: Berlin Heidelberg,  
965 Springer, 535 p. DOI: 10.1007/978-3-642-60423-2

966 Wenger, L. M., C. L. Davis, and G. H. Isaksen, 2001, Multiple controls on petroleum  
967 biodegradation and impact on oil quality: Proceedings SPE Annual Technical  
968 Conference and Exhibition, 14 p. DOI: 10.2118/71450-MS

969 Whalen, M. T., G. P. Eberli, F. S. van Buchem, E. W. Mountjoy, and P. W. Homewood, 2000,  
970 Bypass margins, basin-restricted wedges, and platform-to-basin correlation, Upper

971 Devonian, Canadian Rocky Mountains: implications for sequence stratigraphy of  
972 carbonate platform systems: *Journal of Sedimentary Research*, v. 70, no. 4, p. 913-  
973 936. DOI: 10.1306/2DC40941-0E47-11D7-8643000102C1865D

974 Wu, J., Z. Li, and X. C. Wang, 2016, Comment on “Behavior of Re and Os during contact  
975 between an aqueous solution and oil: Consequences for the application of the Re–Os  
976 geochronometer to petroleum” by Mahdaoui et al. (2015): *Geochimica et*  
977 *Cosmochimica Acta*, v. 186, p. 344-347. DOI: 10.1016/j.gca.2016.02.018

978 Ziegler, W., and C. A. Sandberg, 1990, The Late Devonian standard conodont zonation:  
979 *Courier Forschungsinstitut Senckenberg*, v. 121, 115 p.

980

981 Vitae of authors

982 **Junjie Liu**

983 Department of Earth Sciences, Durham University, Durham, DH1 3LE, UK

984 [junjie.liu@durham.ac.uk](mailto:junjie.liu@durham.ac.uk)

985 Junjie Liu is currently a postdoctoral research associate at Durham University, UK, focusing  
986 on the application and basics of the Re-Os dating of petroleum system. He received his BSc  
987 degree and MSc degree from China University of Geosciences, Beijing, and PhD degree from  
988 Durham University.

989

990 **David Selby**

991 Department of Earth Sciences, Durham University, Durham, DH1 3LE, UK

992 [david.selby@durham.ac.uk](mailto:david.selby@durham.ac.uk)

993 Professor David Selby received his BSc in geology from Southampton University, UK and  
994 PhD from the University of Alberta, Canada, where is also carried out his postdoctoral  
995 research. His research focuses on the application and development of the novel, state-of-the-  
996 art, rhenium-osmium radioisotope methodology to the Earth Science disciplines of economic  
997 geology, petroleum geoscience and paleoclimate and oceanography.

998

999 **Mark Obermajer**

1000 Geological Survey of Canada, Calgary, Alberta, T2L 2A7, Canada

1001 [Mark.Obermajer@NRCan-RNCan.gc.ca](mailto:Mark.Obermajer@NRCan-RNCan.gc.ca)

1002 Mark Obermajer is a scientist at the Geological Survey of Canada, Calgary office. He  
1003 received his MSc degree in geology from Jagiellonian University, Cracow, and a PhD in  
1004 geology from Western University, Ontario. His scientific interest includes organic  
1005 geochemistry of hydrocarbon source rocks, oil-oil and oil-source correlations as applied to  
1006 petroleum systems of Western and Northern Canadian sedimentary basins.

1007

1008 **Andy Mort**

1009 Geological Survey of Canada, Calgary, Alberta, T2L 2A7, Canada

1010 [Andy.Mort@NRCan-RNCan.gc.ca](mailto:Andy.Mort@NRCan-RNCan.gc.ca)

1011 Dr Andy Mort is a research scientist at the Geological Survey of Canada. He has more than  
1012 15 years' experience in conventional and unconventional petroleum systems analysis. His  
1013 repertoire covers molecular geochemistry applied to oil-oil and oil-source correlation,  
1014 thermal history modeling and charge evaluation, biodegradation, reservoir formation damage  
1015 and most recently, the application of geochemistry for fluid phase prediction.

1016

1017

1018

1019 **Figure Captions**

1020 **Figure 1.** Map of the study area showing the location of the oil and Duvernay Formation  
1021 shale samples used in this study (modified from Fowler et al., 2001 with the permission of  
1022 Canadian Society of Petroleum Geologists). The oils are from the Devonian Leduc and Nisku  
1023 formations. The majority of the shale samples are located in the mature zone (16-18-52-5W5,  
1024 14-29-48-6W5, 2-12-50-26W4 and 2-6-47-4W5) with some from the immature zone (10-27-  
1025 57-21W4) and the highly mature zone (1-28-36-3W5 and 8-35-31-25W4). Solvent extracts of  
1026 well 10-27-57-21W4 (low maturity) and 13-14-35-25W4 (high maturity) are used for organic  
1027 geochemical analysis.

1028 **Figure 2.** Devonian stratigraphy of the study area, south-central Alberta (information is  
1029 collectively from the Table of Formations, Alberta by Energy Resources Conservation Board  
1030 based in Calgary, Canada, Aitken and Norris, 2014, Li et al., 1998 and Fowler et al., 2001).  
1031 Late Devonian Woodbend Group Duvernay Formation interfingers with Leduc reefs. Also  
1032 shown here are the organic-rich Devonian-Mississippian Exshaw Formation and the  
1033 equivalent of Middle Devonian Keg River Formation, the Winnipegosis Formation.

1034 **Figure 3.** Migration of the Duvernay Formation generated oil (Modified from Switzer et al.,  
1035 1994 and Rostron, 1997). Following oil generation the Duvernay oil migrated to adjacent  
1036 Leduc reefs with the underlying Cooking Lake carbonates working as a “pipe line”. In the  
1037 Bashaw reef area, the differential compaction of the Ireton aquitard due to the underlying  
1038 Leduc reefs leads to the thinning or absence of the aquitard. This facilitates the breach of  
1039 Duvernay sourced oil from Leduc reefs to the overlying Nisku formation.

1040 **Figure 4.** Asphaltene content versus asphaltene Re (ppb) and unradiogenic Os (ppt,  
1041 represented by  $^{192}\text{Os}$ ) abundance of the Duvernay oils.

1042 **Figure 5.**  $^{187}\text{Re}/^{188}\text{Os}$  vs  $^{187}\text{Os}/^{188}\text{Os}$  plot for the asphaltene fractions of the Duvernay oil. See  
1043 text for discussion.

1044 **Figure 6.** The individually calculated  $\text{Os}_i$  values of asphaltene samples of the Duvernay oil.  
1045 determined at 66 Ma.

1046 **Figure 7.** Duvernay Formation total organic carbon (TOC) (Stasiuk and Fowler, 2002), Re  
1047 and unradiogenic Os ( $^{192}\text{Os}$  as representative) abundances, and calculated  $^{187}\text{Os}/^{188}\text{Os}$   
1048 compositions at the time of deposition ( $\text{Os}_i$ , 378.5 Ma) and oil generation ( $\text{Os}_g$ , 66 Ma). The  
1049 depth of TOC does not correlate exactly with the Re and Os data (Fowler et al., 2003).  
1050 Broadly the Re and Os abundances positively co-vary with the TOC content. The  $\text{Os}_i$  values  
1051 show a limited (0.28 to 0.38) range, and yield a weighted average of  $\sim 0.33$ , reflecting a  
1052 relatively nonradiogenic  $^{187}\text{Os}/^{188}\text{Os}$  composition for contemporaneous seawater. The  $\text{Os}_g$   
1053 values of the Duvernay Formation calculated at 66 Ma are between 0.46 and 1.48, and yield a  
1054 Tukey's Biweight mean of  $0.833 \pm 0.009$ .

1055 **Figure 8a.** Representative gas chromatograms showing distributions of: 1) gasoline range  
1056 hydrocarbons and 2) normal alkanes and isoprenoids in low (sample L02221), medium  
1057 (sample L02155) and high (sample L02177) maturity Duvernay-sourced crude oils. The high  
1058 maturity oils have very low asphaltene content and hence were not selected for Re-Os  
1059 analysis. For peak annotations see Table 4.

1060 **Figure 8b.** Representative gas chromatograms showing distributions of: 3) terpanes and 4)  
1061 steranes in low (sample L02221), medium (sample L02155) and high (sample L02177)  
1062 maturity Duvernay-sourced crude oils.

1063

1064 **Figure 9.** Histogram showing distribution of total organic carbon (TOC) content in the  
1065 Duvernay Formation samples.

1066

1067 **Figure 10.** A cross-plot of Rock-Eval hydrogen (HI) and oxygen (OI) indices for the 4 wells  
1068 from which Re-Os data were collected during present study. The data indicate presence of  
1069 Type I-II organic matter in most of the samples; notice a systematic decrease in HI values  
1070 corresponding to an increase in thermal maturity levels from 10-27-57-21W4 and 16-18-52-  
1071 5W5 through 14-29-48-6W5 to 2-6-47-4W5.

1072

1073 **Figure 11.** Extract yield data showing relative maturity and source rock potential of the  
1074 Duvernay Formation samples (criteria by Powell, 1978).

1075

1076 **Figure 12.** Saturate fraction gas chromatograms showing distributions of 1) normal alkanes  
1077 and isoprenoids, 2) terpanes and 3) steranes in low and high maturity Duvernay Formation  
1078 organic extracts. For peak annotations see Table 4.

1079 **Figure 13.** Oil-source correlation of a Nisku crude oil from Wood River field (within the  
1080 Bashaw reef complex, 10-28-42-23W4, sample L02203) and Duvernay Formation organic

1081 extract from 13-14-35-25W4 showing strong similarities in the distributions of terpane and  
1082 sterane biomarkers. For peak annotations see Table 4.

1083

1084 **Figure 14.** Ternary diagram showing relative normalized abundance of C<sub>27</sub>:C<sub>28</sub>:C<sub>29</sub> regular  
1085 steranes based on  $\alpha\beta\beta$  isomers in the analyzed oil samples. Data for 29 Duvernay extracts  
1086 (from GSC-C database) are shown for comparison.

1087 **Figure 15.**  $^{187}\text{Re}/^{188}\text{Os}$  vs  $^{187}\text{Os}/^{188}\text{Os}$  plots for the Duvernay formation. A) core 10-27-57-  
1088 21W4; B) core 16-18-52-5W5; C) core 14-29-48-6W5; D) core 2-6-47-4W5; and E) all data  
1089 including samples from references (Selby et al., 2007; Finlay et al., 2012). See text for  
1090 discussion.

1091 **Figure 16.** Comparison of the currently available  $^{187}\text{Os}/^{188}\text{Os}$  compositions at 66 Ma for the  
1092 WCSB Phanerozoic organic-rich intervals shown with the Duvernay shale  $\text{Os}_g$  and oil  $\text{Os}_i$   
1093 values.

1094

1095 **Table 1.** Well locations and reservoir formations of the oil samples of this study

1096 **Table 2.** Re-Os data synopsis for the Duvernay Formation shale samples from multiple  
1097 locations (wells) and their  $\text{Os}_i$  (378.5 Ma) and  $\text{Os}_g$  (66 Ma) values

1098 **Table 3.** Re-Os data synopsis for asphaltene fractions of the oil samples from the Duvernay  
1099 petroleum system and their  $\text{Os}_i$  (66 Ma) values.

1100 **Table 4.** The compounds represented by the peak annotations in the geochemistry figures

1101 (Fig. 8, 12 and 13)

1102 **Table 5.** Re-Os data and calculated  $^{187}\text{Os}/^{188}\text{Os}$  composition at 66 Ma for other oil prone

1103 strata of the WCSB.

Table 1 Well locations and reservoir formations of the oil samples of this study

Sample ID	Well ID	Latitude	Longitude	Depth (m)	Depth (ft)	Formation
L00864	14-35-48-27W4	53.19	-113.85	1920.0-1923.9	6299.2-6312.0	Leduc
L00873	10-9-48-27W4	53.13	-113.89	1781.9-1783.4	5846.1-5851.0	Nisku
L01558	01-3-37-20W4	52.15	-112.77	1604.8-1622.1	5265.1-5321.9	Nisku
L01810	12-11-49-12W5	53.21	-115.66	2997-3069	9833-10069	Nisku
L01827	11-14-42-2W5	52.62	-114.18	2373-2387	7785-7831	Leduc
L01831	8-35-48-12W5	53.18	-115.64	3059-3086	10036-10125	Nisku
L02037	16-16-41-2W5	52.54	-114.22	2431-2442	7976-8012	Nisku
L02083	12-13-41-23W4	52.53	-113.19	1742-1743	5715-5719	Nisku
L02155	10-31-39-23W4	52.4	-113.3	1781.3	5844.2	Nisku
L02196	9-11-33-26W4	51.81	-113.59	2497.8	8194.9	Leduc
L02197	9-14-33-26W4	51.83	-113.58	2202	7224	Nisku
L02203	10-28-42-23W4	52.65	-113.25	1720	5643	Nisku
L02220	11-35-36-20W4	52.14	-112.76	1606.3	5270.0	Nisku
L02221	7-23-36-20W4	52.1	-112.75	1569.7-1617.9	5149.9-5308.1	Leduc/Nisku
L02225	15-22-38-20W4	52.29	-112.78	1563.6-1645.9	5129.9-5399.9	Leduc
L02226	12-10-38-20W4	52.25	-112.79	1569.7-1624.6	5149.9-5330.1	Leduc
L01822	2-27-37-20W4	52.2	-112.78	1599-1603	5246-5259	Leduc

Table 2 Re-Os data synopsis for the Duvernay Formation shale samples from multiple well locations

Sample	Depth (m)	Depth (ft)	Re (ppb) ±	Os (ppt) ±	<sup>192</sup> Os (ppt) ±	<sup>187</sup> Re/ <sup>188</sup> Os ±	<sup>187</sup> Os/ <sup>188</sup> Os ±	rho <sup>a</sup>	Os <sub>i</sub> <sup>b</sup> ±	Os <sub>g</sub> <sup>c</sup> ±
<i>10-27-57-21W4</i>			<i>53.96°N</i>		<i>113.03°W</i>					
DS18-12	1106	3629	5.84 ± 0.02	631.2 ± 2.2	244.5 ± 1.0	47.5 ± 0.2	0.633 ± 0.004	0.590	0.33 ± 0.01	0.58 ± 0.01
DS20-12	1125	3691	14.37 ± 0.04	1245.3 ± 4.8	478.7 ± 2.2	59.7 ± 0.3	0.693 ± 0.005	0.604	0.32 ± 0.01	0.63 ± 0.01
DS22-12	1128	3701	13.23 ± 0.04	1299.2 ± 5.1	500.7 ± 2.4	52.5 ± 0.3	0.673 ± 0.005	0.600	0.34 ± 0.01	0.62 ± 0.01
DS24-12	1140	3740	12.36 ± 0.04	1121.1 ± 4.4	431.3 ± 2.1	57.0 ± 0.3	0.687 ± 0.005	0.600	0.33 ± 0.01	0.62 ± 0.01
DS26-12	1144	3753	16.86 ± 0.05	947.8 ± 3.8	355.5 ± 1.5	94.4 ± 0.5	0.899 ± 0.005	0.598	0.30 ± 0.01	0.80 ± 0.01
DS28-12	1146	3760	14.68 ± 0.04	1392.9 ± 5.2	537.7 ± 2.4	54.3 ± 0.3	0.659 ± 0.004	0.598	0.32 ± 0.01	0.60 ± 0.01
DS30-12	1151	3776	26.33 ± 0.07	1965.2 ± 6.9	751.1 ± 2.9	69.8 ± 0.3	0.742 ± 0.004	0.584	0.30 ± 0.01	0.67 ± 0.01
DS32-12	1154	3786	24.15 ± 0.06	1537.6 ± 5.6	579.5 ± 2.2	82.9 ± 0.4	0.859 ± 0.005	0.582	0.34 ± 0.01	0.77 ± 0.01
DS34-12	1160	3806	10.91 ± 0.03	397.1 ± 2.0	142.7 ± 0.7	152.0 ± 0.9	1.267 ± 0.009	0.608	0.31 ± 0.02	1.10 ± 0.01
DS36-12	1161	3809	25.43 ± 0.07	1188.0 ± 4.7	436.5 ± 1.7	115.9 ± 0.5	1.074 ± 0.006	0.582	0.34 ± 0.01	0.95 ± 0.01
<i>16-18-52-5W5</i>			<i>53.5°N</i>		<i>114.72°W</i>					
DS1-12	2343.0	7687.0	0.31 ± 0.01	58.8 ± 2.1	23.2 ± 1.9	26.3 ± 2.2	0.488 ± 0.055	0.687	0.32 ± 0.07	0.46 ± 0.06
DS3-12	2343.5	7689.6	1.25 ± 0.01	242.5 ± 2.5	95.6 ± 1.9	26.0 ± 0.5	0.491 ± 0.014	0.683	0.33 ± 0.02	0.46 ± 0.02
DS5-12	2344.0	7690.3	2.03 ± 0.01	178.1 ± 1.3	68.5 ± 0.8	58.9 ± 0.7	0.693 ± 0.012	0.671	0.32 ± 0.02	0.63 ± 0.01
DS7-12	2344.5	7691.9	4.03 ± 0.01	248.0 ± 1.3	93.4 ± 0.7	85.8 ± 0.7	0.862 ± 0.009	0.657	0.32 ± 0.01	0.77 ± 0.01
<i>14-29-48-6W5</i>			<i>53.18°N</i>		<i>114.85°W</i>					
DS9-12	2646.6	8683.1	48.46 ± 0.14	1370.7 ± 8.2	474.1 ± 2.9	203.3 ± 1.4	1.611 ± 0.014	0.646	0.32 ± 0.02	1.39 ± 0.02
DS11-12	2648.6	8689.6	8.75 ± 0.03	362.4 ± 1.9	132.7 ± 0.8	131.3 ± 0.9	1.107 ± 0.010	0.622	0.28 ± 0.02	0.96 ± 0.01
DS13-12	2650.6	8696.2	10.82 ± 0.03	482.0 ± 2.3	176.0 ± 0.9	122.3 ± 0.7	1.129 ± 0.008	0.609	0.36 ± 0.01	0.99 ± 0.01
DS15-12	2652.6	8702.8	21.94 ± 0.06	1827.3 ± 6.6	700.6 ± 2.8	62.3 ± 0.3	0.716 ± 0.004	0.576	0.32 ± 0.01	0.65 ± 0.01
DS17-12	2654.6	8709.3	36.35 ± 0.09	1726.5 ± 8.7	636.2 ± 3.4	113.7 ± 0.7	1.050 ± 0.009	0.589	0.33 ± 0.01	0.93 ± 0.01

<i>2-6-47-4W5</i>			<i>53.02°N</i>		<i>114.57°W</i>												
DS37-12	2629	8625	0.53	0.01	29.0	1.0	10.8	0.9	98.2	8.0	0.942	0.107	0.701	0.32	0.16	0.83	0.12
DS38-12	2631	8632	0.40	0.01	30.7	0.7	11.7	0.6	68.2	3.6	0.792	0.056	0.677	0.36	0.08	0.72	0.06
DS39-12	2633	8638	1.36	0.01	62.2	0.9	22.8	0.6	118.5	3.2	1.110	0.042	0.694	0.36	0.06	0.98	0.05
DS40-12	2635	8645	41.52	0.14	1218.3	4.2	423.1	1.0	195.2	0.8	1.575	0.005	0.403	0.34	0.01	1.36	0.01
DS41-12	2637	8652	67.56	0.22	1721.5	7.0	587.5	1.7	228.8	1.0	1.736	0.007	0.476	0.29	0.01	1.48	0.01
DS42-12	2639	8658	13.07	0.04	900.4	2.9	340.3	1.1	76.4	0.3	0.836	0.004	0.486	0.35	0.01	0.75	0.01
DS43-12	2641	8665	11.27	0.04	746.9	3.7	282.3	1.8	79.4	0.6	0.835	0.007	0.620	0.33	0.01	0.75	0.01
DS44-12	2643	8671	5.99	0.02	430.7	1.8	163.0	0.8	73.1	0.4	0.823	0.006	0.576	0.36	0.01	0.74	0.01
DS45-12	2645	8678	8.74	0.03	598.6	3.5	226.1	1.8	76.9	0.7	0.841	0.010	0.648	0.35	0.01	0.76	0.01
DS46-12	2647	8684	28.75	0.09	1707.7	5.7	639.0	2.0	89.5	0.4	0.919	0.004	0.482	0.35	0.01	0.82	0.01
DS47-12	2649	8691	41.79	0.14	1774.0	8.1	649.0	3.1	128.1	0.7	1.112	0.008	0.581	0.30	0.01	0.97	0.01
<i>2-12-50-26W4<sup>d</sup></i>			<i>53.30°N</i>		<i>113.67°W</i>												
DS44-03	1751.6	5746.7	7.41	0.03	383	2	140	1	104.4	0.6	1.037	0.006	0.800	0.38	0.01	0.92	0.01
<i>8-35-31-25W4<sup>d</sup></i>			<i>51.70°N</i>		<i>113.43°W</i>												
DS69-03	2340.9	7680.1	11.55	0.04	569	2	208	1	109.5	0.5	1.036	0.004	0.800	0.34	0.01	0.92	0.01
<i>1-28-36-3W5<sup>e</sup></i>			<i>52.20°N</i>		<i>114.60°W</i>												
DS45-03-1-4	3013.1	9885.5	8.10	0.03	219.6	1.2	75.3	0.4	214.1	1.2	1.689	0.012	0.542	0.34	0.02	1.45	0.01

<sup>a</sup> rho: error correlation value between <sup>187</sup>Re/<sup>188</sup>Os and <sup>187</sup>Os/<sup>188</sup>Os;

<sup>b</sup> Os<sub>i</sub> = initial <sup>187</sup>Os/<sup>188</sup>Os ratio of shales during deposition which is calculated at 378.5 Ma (see text for discussion);

<sup>c</sup> Os<sub>g</sub> = <sup>187</sup>Os/<sup>188</sup>Os ratio of shales at oil generation calculated at 66 Ma (see text for discussion);

<sup>d</sup> Data from Finlay et al. (2012);

<sup>e</sup> Data from Selby et al. (2007).

Table 3 Re-Os data synopsis for asphaltene fractions of the oil samples from the Duvernay petroleum system

Sample ID	Asphaltene (%)	Re (ppb)	±	Os (ppt)	±	<sup>192</sup> Os (ppt)	±	<sup>187</sup> Re/ <sup>188</sup> Os	±	<sup>187</sup> Os/ <sup>188</sup> Os	±	rho <sup>a</sup>	Os <sub>i</sub> <sup>b</sup>	±
L00864	1.61%	0.12	0.07	9.4	0.5	3.6	0.5	66.8	37.1	0.775	0.111	0.211	0.70	0.15
L00864rpt	1.16%	0.13	0.05	8.2	0.4	3.0	0.3	84.9	31.1	0.980	0.118	0.270	0.89	0.15
L00864rpt2	1.81%	0.12	0.04	7.4	0.4	2.7	0.4	84.1	32.0	1.036	0.164	0.291	0.94	0.20
L00873	5.65%	0.42	0.03	8.8	0.3	3.3	0.2	256.1	26.1	1.006	0.086	0.621	0.72	0.12
L01558	3.60%	1.42	0.03	20.4	0.5	7.6	0.4	371.1	20.0	0.970	0.063	0.698	0.56	0.09
L02083	2.46%	1.26	0.04	11.2	0.4	3.9	0.3	641.6	51.8	1.521	0.131	0.814	0.82	0.19
L02155	1.45%	0.32	0.04	3.6	0.3	1.2	0.3	511.4	131.1	1.623	0.373	0.844	1.06	0.52
L02196	0.25%	0.04	0.00	0.6	0.1	0.2	0.1	351.4	81.0	1.105	0.275	0.918	0.72	0.36
L02203	1.39%	0.26	0.00	4.6	0.5	1.7	0.5	298.8	85.4	0.878	0.273	0.919	0.55	0.37
L02220	3.00%	1.41	0.03	19.1	0.5	7.0	0.4	400.4	22.9	1.105	0.073	0.712	0.66	0.10
L02221 <sup>c</sup>	14.10%	3.78	0.04	41.2	1.6	14.9	1.2	504.7	42.3	1.206	0.139	0.712	0.65	0.19
L02225 <sup>c</sup>	6.75%	0.51	0.04	6.4	0.4	2.3	0.3	442.6	74.5	1.285	0.219	0.760	0.80	0.30
L02226 <sup>c</sup>	5.84%	1.11	0.05	12.0	0.6	4.2	0.5	524.6	68.6	1.475	0.216	0.766	0.90	0.29
L01822 <sup>d</sup>	14.50%	2.03	0.07	25.3	1.6	8.8	0.6	457.1	72.3	1.488	0.236	0.500	0.99	0.32
Data not applied on isochron														
L01810	0.35%	0.04	0.11	1.0	0.8			218.2	705.6	0.63	1.33	0.54		
L01831	0.52%	0.01	0.11	23.3	1.0			2.0	25.1	1.11	0.12	0.01		
L02196rpt	0.78%	0.02	0.05	0.6	0.4			210.4	562.6	0.52	0.92	0.51		
L02037	0.28%	0.05	0.17	-	-			-	-	-	-	-		
L02197	0.27%	0.07	0.17	-	-			-	-	-	-	-		

<sup>a</sup> rho: error correlation value between <sup>187</sup>Re/<sup>188</sup>Os and <sup>187</sup>Os/<sup>188</sup>Os;

<sup>b</sup> Os<sub>i</sub> = initial <sup>187</sup>Os/<sup>188</sup>Os ratios of oil at the timing of generation which are calculated at 66 Ma (see text for discussion);

<sup>c</sup> these samples are asphaltene fractions precipitated by *n*-pentane at the GSC;

<sup>d</sup> data from Selby et al. (2007).

Table 4 The compounds represented by the peak annotations in the geochemistry figures (Fig. 8-10)

<b>Peak</b>	<b>Compound</b>	<b>Peak</b>	<b>Compound</b>
<i>n</i> -C <sub>5</sub>	C <sub>5</sub> <i>n</i> -alkane	C <sub>26</sub> TT	C <sub>26</sub> tricyclic terpane
<i>n</i> -C <sub>6</sub>	C <sub>6</sub> <i>n</i> -alkane	Ts	18 $\alpha$ (H),22,29,30-trisnorhopane (Ts)
MCYC5	methylcyclopentane	Tm	17 $\alpha$ (H),22,29,30-trisnorhopane (Tm)
<i>n</i> -C <sub>7</sub>	C <sub>7</sub> <i>n</i> -alkane	C <sub>29</sub>	17 $\alpha$ (H),21 $\beta$ (H)-30-norhopane
MCYC6	methylcyclohexane	C <sub>29</sub> Ts	18 $\alpha$ (H),21 $\beta$ (H)-norneohopane
<i>n</i> -C <sub>8</sub>	C <sub>8</sub> <i>n</i> -alkane	C <sub>30</sub> H	17 $\alpha$ (H),21 $\beta$ (H)-hopane
Pr	pristane	G	gammacerane
Ph	phytane	C <sub>34</sub>	17 $\alpha$ (H),21 $\beta$ (H)-tetrakishomohopanes
<i>n</i> -C <sub>15</sub>	C <sub>15</sub> <i>n</i> -alkane	C <sub>35</sub>	17 $\alpha$ (H),21 $\beta$ (H)-pentakishomohopanes
<i>n</i> -C <sub>20</sub>	C <sub>20</sub> <i>n</i> -alkane	C <sub>21</sub> P	pregnane
<i>n</i> -C <sub>25</sub>	C <sub>25</sub> <i>n</i> -alkane	dC <sub>27</sub> S20S	diacholestane 20S
C <sub>23</sub> TT	C <sub>23</sub> tricyclic terpane	dC <sub>29</sub> S20S	diastigmastane 20S
C <sub>24</sub> TeT	C <sub>24</sub> tetracyclic terpane	C <sub>29</sub> S20R	5 $\alpha$ (H),14 $\beta$ (H),17 $\beta$ (H)-stigmastane 20R

Table 5 Re-Os data and calculated  $^{187}\text{Os}/^{188}\text{Os}$  composition at 66 Ma ( $\text{Os}_g$ ) for other oil prone strata of the WCSB

**Lower Jurassic Gordondale Member**

*Finlay et al. (2012)*

wells	depth (m)	depth (ft)	Re (ppb)	Os (ppt)	$^{187}\text{Re}/^{188}\text{Os}$	$^{187}\text{Os}/^{188}\text{Os}$	$\text{Os}_g^a$
07-31-79-10W6	1557.0	5108.3	574.9	6.34	550.4	2.116	1.51
14-24-80-7W6	1183.5	3882.9	369.2	1.86	1674	5.900	4.06
14-24-80-7W6	1190.4	3905.5	229.9	1.83	885.8	3.655	2.68
8-26-69-7W6	2271.4	7452.1	195.3	6.13	178.6	1.372	1.18
10-17-84-22W5	2361.0	7746.1	196.2	1.12	1352	4.748	3.26
6-29-85-11W5	1148.7	3768.7	402.6	3.05	933.2	3.716	2.69

*Selby et al. (2007)<sup>b</sup>* well 6-32-78-5W6 1218.0-1218.6 m (3996.1-3998.0 ft)

sample	$^{187}\text{Re}/^{188}\text{Os}$	$^{187}\text{Os}/^{188}\text{Os}$	$\text{Os}_g^a$
TS22b.DD.GB	765.25	2.925	2.08
TS23c.DD.GB	432.40	1.914	1.44
TS24b.DD.GB	291.71	1.405	1.08
TS25b.DD.GB	424.18	1.926	1.46
TS26a.DD.GB	182.21	1.186	0.99

**Devonian-Mississippian Exshaw Formation**

*Selby and Creaser (2005)* 51°05'29"N 115°09'29"W

within ~4 m (13 ft) lateral interval and 10 cm (0.4 in) of vertical stratigraphy

sample	Re (ppb)	Os (ppt)	$^{187}\text{Re}/^{188}\text{Os}$	$^{187}\text{Os}/^{188}\text{Os}$	$\text{Os}_g^a$
DS53	15.6	367.8	253.5	1.948	1.67
DS54	17.5	375.9	283.8	2.141	1.83
DS55A	15.5	341.4	273.7	2.073	1.77
DS55B	16.4	363.5	277.3	2.100	1.80
DS55C	21.2	426.3	306.1	2.265	1.93
DS56	16.4	493.3	190.4	1.570	1.36
DS57	36.0	595.8	391.8	2.787	2.36
DS58A	15.2	458.7	189.3	1.563	1.35
DS58B	16.6	490.6	194.5	1.597	1.38

*Selby et al. (2003); Creaser et al. (2002); Finlay et al. (2012)*

wells	depth (m)	depth (ft)	Re (ppb)	Os (ppb)	$^{187}\text{Re}/^{188}\text{Os}$	$^{187}\text{Os}/^{188}\text{Os}$	$\text{Os}_g^a$
3-19-80-23W5	1752.0	5748.0	70.0	0.69	487.1	3.517	2.98
3-19-80-23W5	1753.0	5751.3	88.8	1.62	350.7	2.656	2.27
3-19-80-23W5	1754.0	5754.6	22.8	0.50	279.8	2.195	1.89
3-19-80-23W5	1756.5	5762.8	31.7	0.48	441.1	3.220	2.73
13-18-80-23W5	1748.8	5737.5	47.9	0.64	518.3	3.546	2.98
13-18-80-23W5	1750.9	5744.4	68.9	1.11	408.9	2.987	2.54
8-29-78-01W6	2099.1	6886.8	128.6	1.70	538.4	3.806	3.21

8-29-78-01W6	2099.2	6887.1	20.0	0.69	166.1	1.535	1.35
14-22-80-02W6	2058.3	6753.0	31.8	0.67	287.5	2.095	1.78
6-19-78-25W5	2006.2	6582.0	52.0	0.84	405.1	2.885	2.44
4-23-72-10W6	3570.4	11713.9	31.3	0.29	916.8	5.968	4.96
4-23-72-10W6	3567.7	11705.1	42.3	0.80	327.8	2.389	2.03

### Middle Devonian Keg River Formation, La Crete Basin

Miller (2004)

sample ID	Re (ppb)	Os (ppb)	$^{187}\text{Re}/^{188}\text{Os}$	$^{187}\text{Os}/^{188}\text{Os}$	$\text{Os}_g^a$
CM-KR-1	50.8	1.24	238	1.775	1.51
CM-KR-2	34.6	0.94	208	1.568	1.34
CM-KR-3	32.8	0.92	204	1.575	1.35
CM-KR-4	20.7	0.47	259	1.920	1.64
CM-KR-5	57.2	0.95	386	2.733	2.31
CM-KR-6	224.2	2.32	757	5.087	4.25
CM-KR-7	26.7	0.67	232	1.754	1.50
CM-KR-I-D	42.4	0.78	336	2.392	2.02
CM-KR-I-E	37.9	0.78	294	2.124	1.80

### Ordovician Kukersites, Williston Basin

Miller (2004)

sample ID	Re (ppb)	Os (ppb)	$^{187}\text{Re}/^{188}\text{Os}$	$^{187}\text{Os}/^{188}\text{Os}$	$\text{Os}_g^a$
CM-13	2.60	0.085	146	1.608	1.45
CM-14	0.94	0.033	136	1.390	1.24
CM-15	1.01	0.031	155	1.742	1.57
CM-16 (rpt.)	0.60	0.069	44.7	0.776	0.73
CM-17 (rpt.)	0.27	0.074	18.5	0.476	0.46
CM-19 (rpt.)	0.40	0.063	31.4	0.514	0.48
CM-22 (rpt.)	0.40	0.067	30.2	0.580	0.55
CM-IV-A-iii.iv.v (rpt.)	0.22	0.019	54.7	0.899	0.84
CM-IV-A-v,vi,vii (rpt.)	0.24	0.023	50	0.894	0.84
CM-IV-A-xiii,xiv,xv	0.23	0.015	75.6	0.943	0.86
CM-IV-A-xvi	0.14	0.030	22.4	0.593	0.57
CM-24	6.58	0.070	752	6.190	5.36
CM-28	0.50	0.048	49.5	0.845	0.79

### Neoproterozoic Old Fort Point Formation, Jasper, Alberta

Kendall et al. (2004)

52.96°N 118.48°W

samples	Re (ppb)	Os (ppt)	$^{187}\text{Re}/^{188}\text{Os}$	$^{187}\text{Os}/^{188}\text{Os}$	$\text{Os}_g^a$	$\text{Os}_i^c$
BK-01-014B	15.43	249.4	524.7	5.954	5.38	0.61
BK-01-015A	6.36	164.7	262.9	3.299	3.01	0.62
BK-01-015B	12.53	218.9	463.7	5.352	4.84	0.63
BK-01-015C	8.54	192.0	318.7	3.859	3.51	0.61
BK-01-015D	7.28	144.8	379.6	4.475	4.06	0.61

<sup>a</sup>  $Os_g = {}^{187}Os/{}^{188}Os$  ratios of strata at the approximate timing of thermal maturation of most of the strata (adopting the Re-Os age of 66 Ma);

<sup>b</sup> No Re and Os abundance data available;

<sup>c</sup>  $Os_i$  = initial  ${}^{187}Os/{}^{188}Os$  ratios of Old Fort Point Formation calculated at its Re-Os depositional age of 608 Ma.

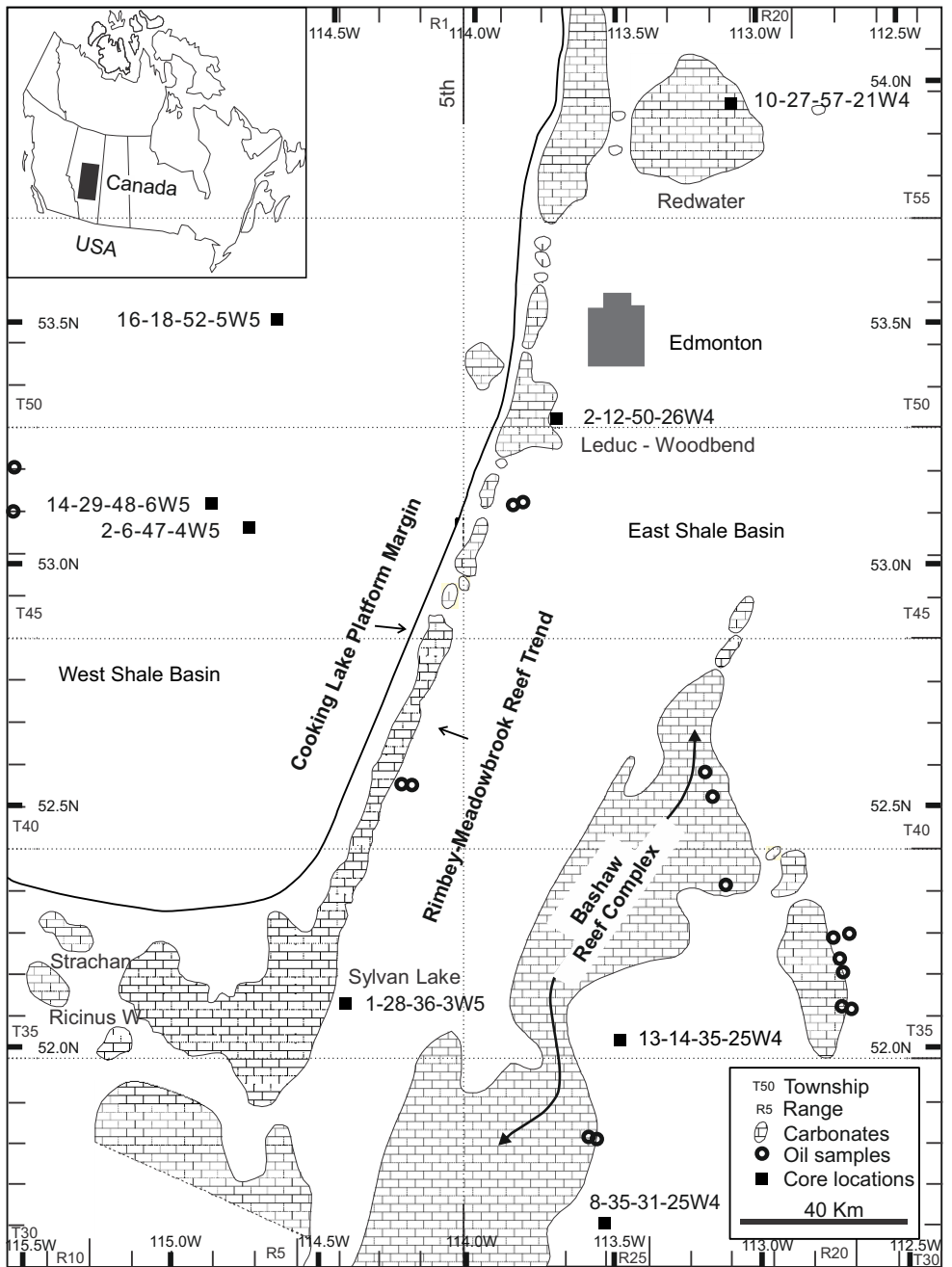


Figure 1

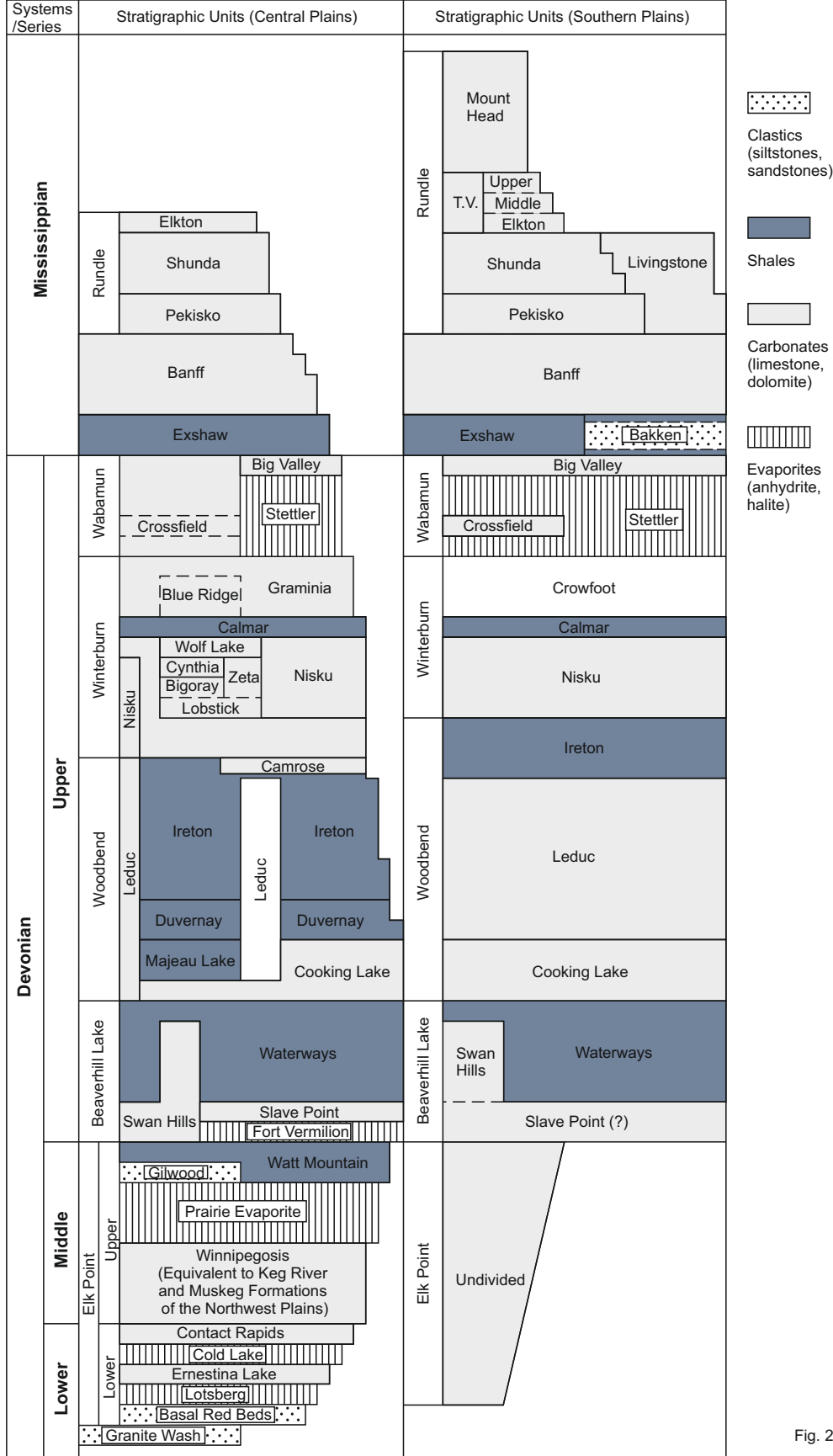


Fig. 2

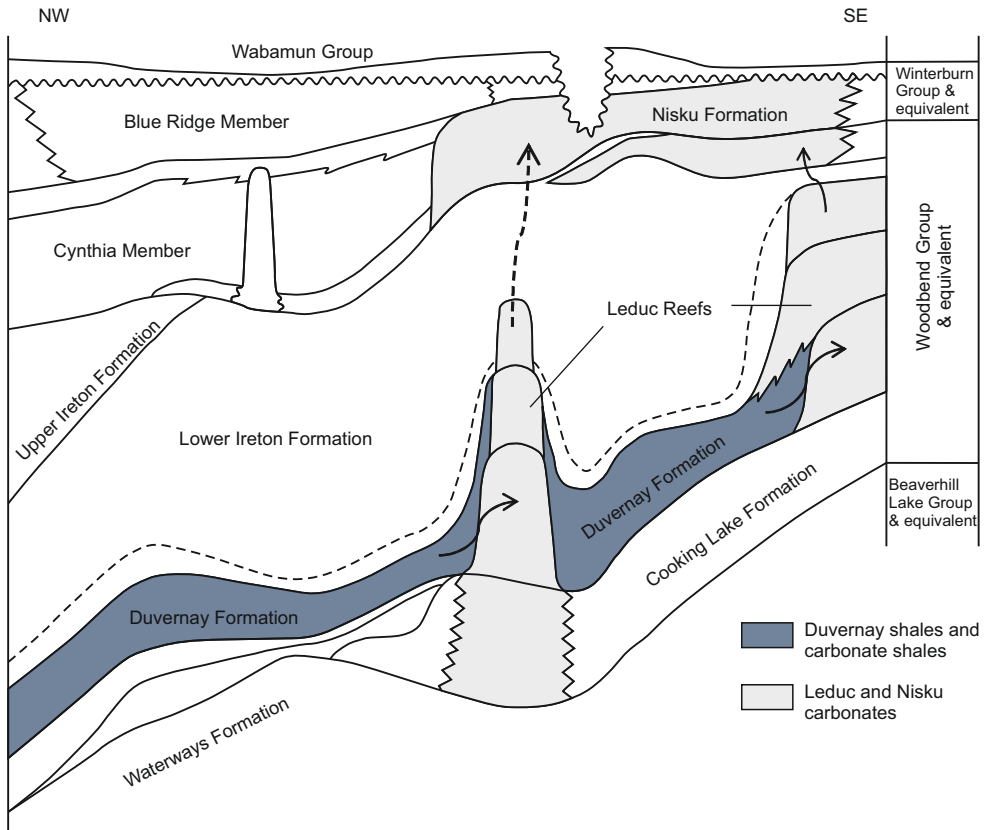


Figure 3

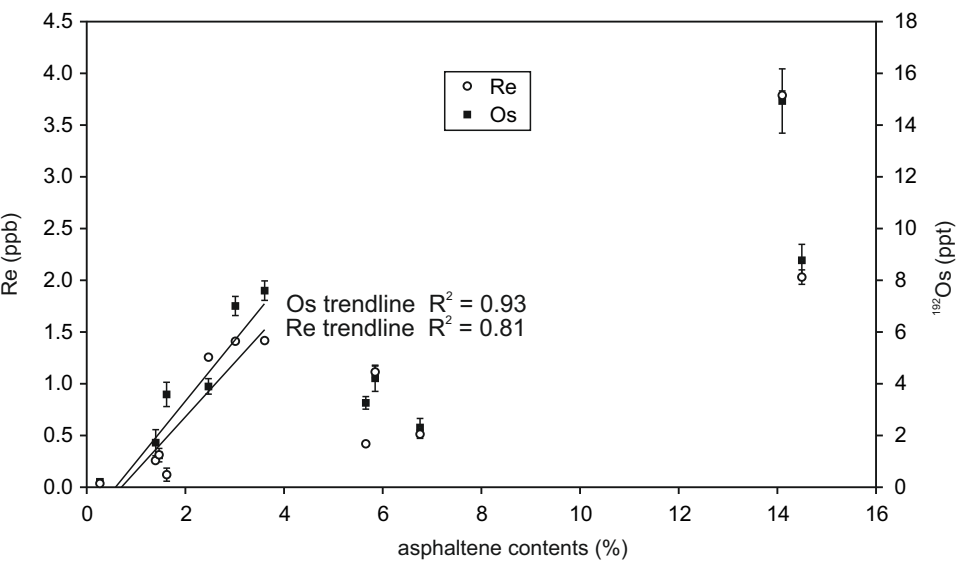


Figure 4

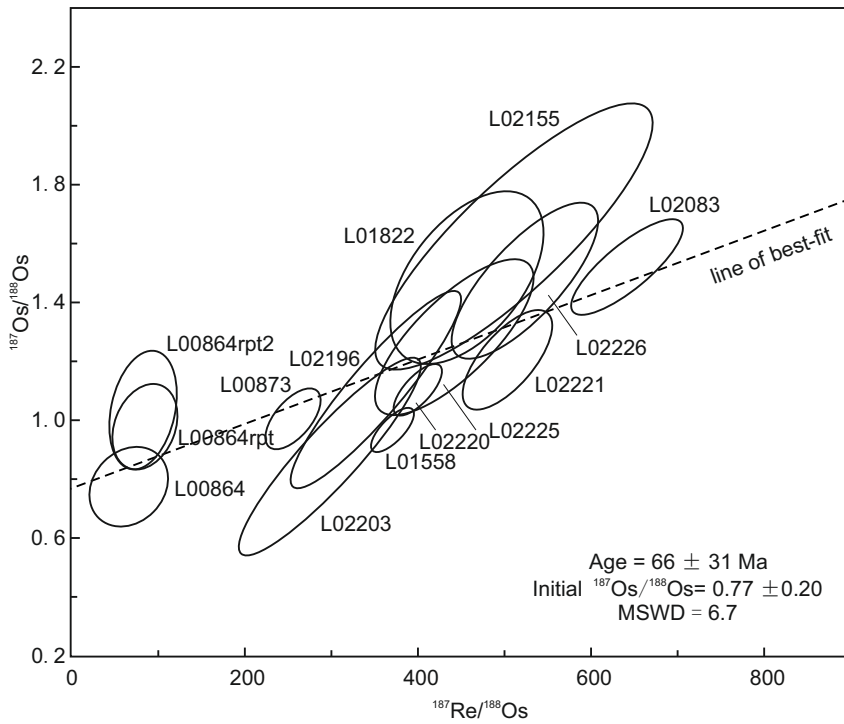


Figure 5

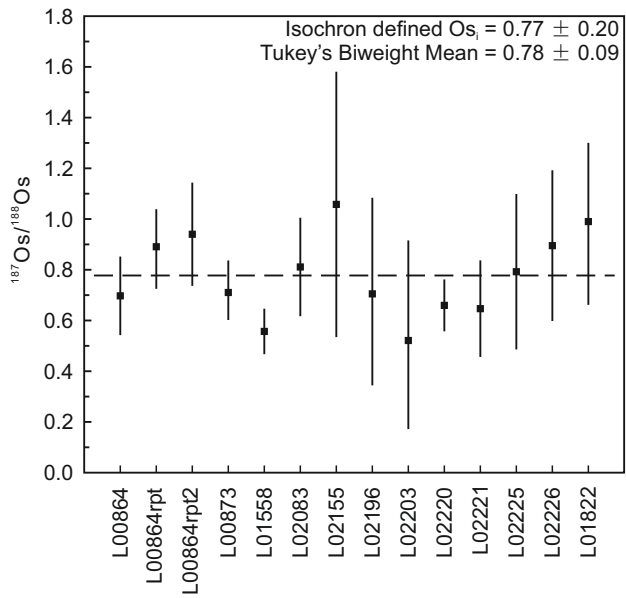
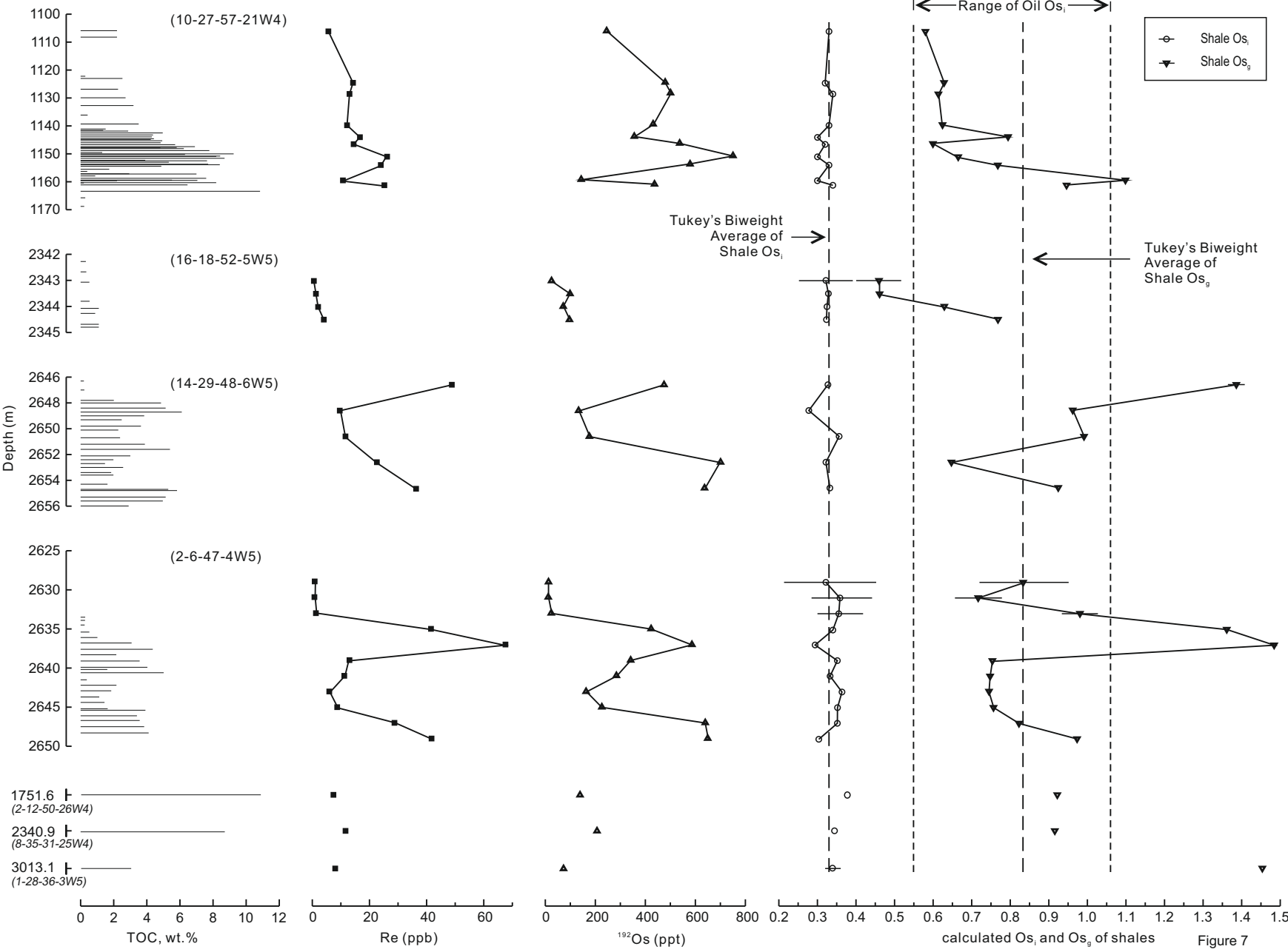


Figure 6



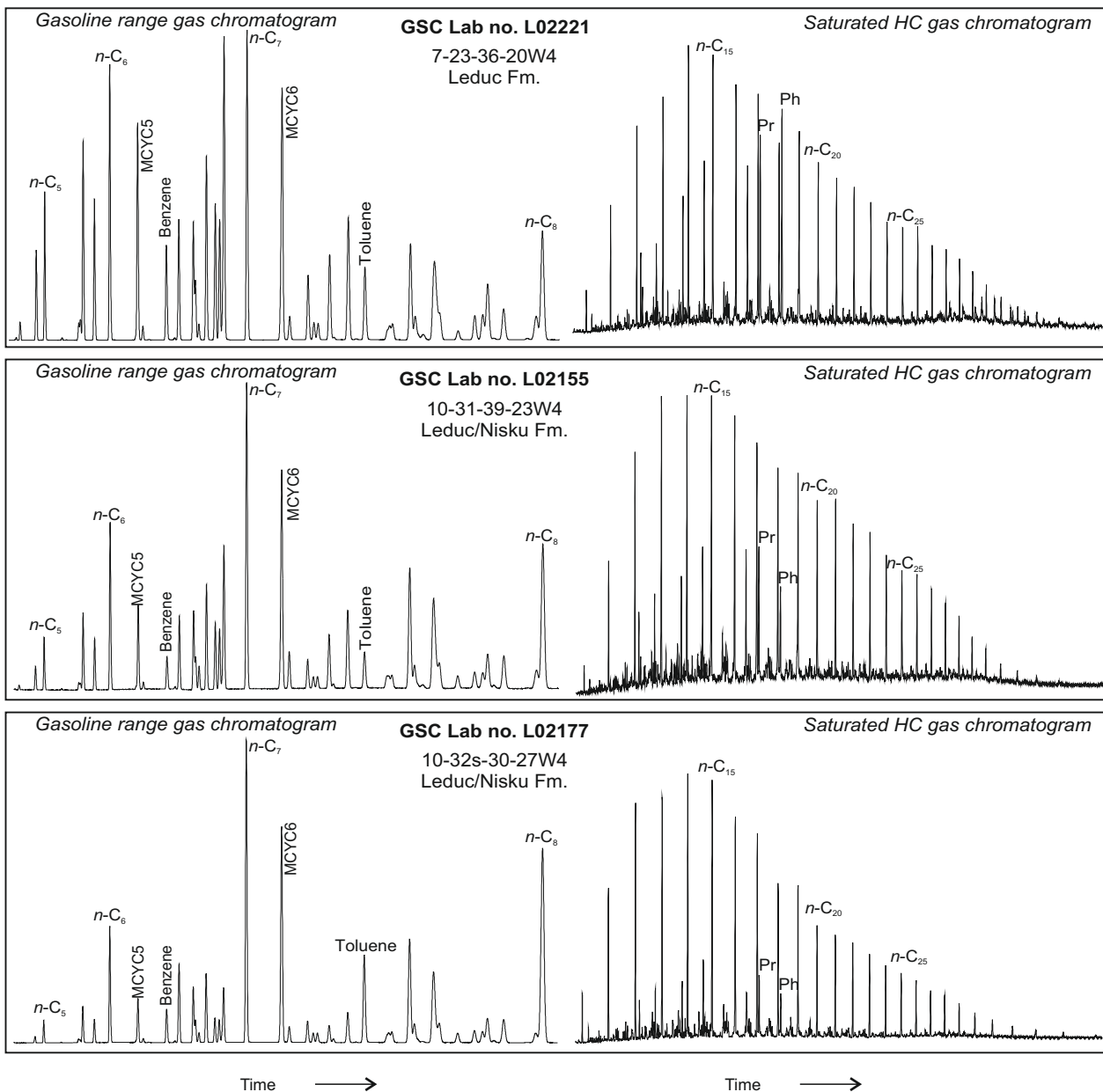


Figure 8a

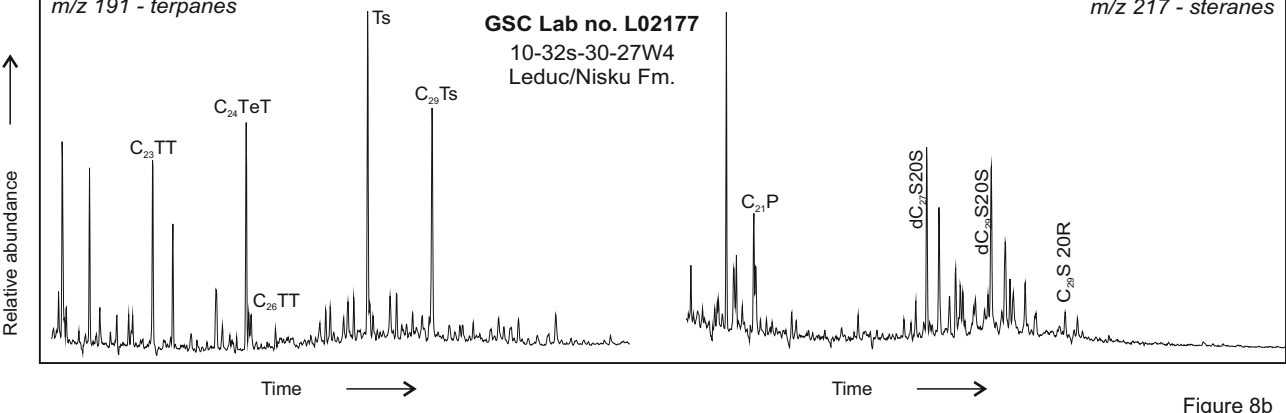
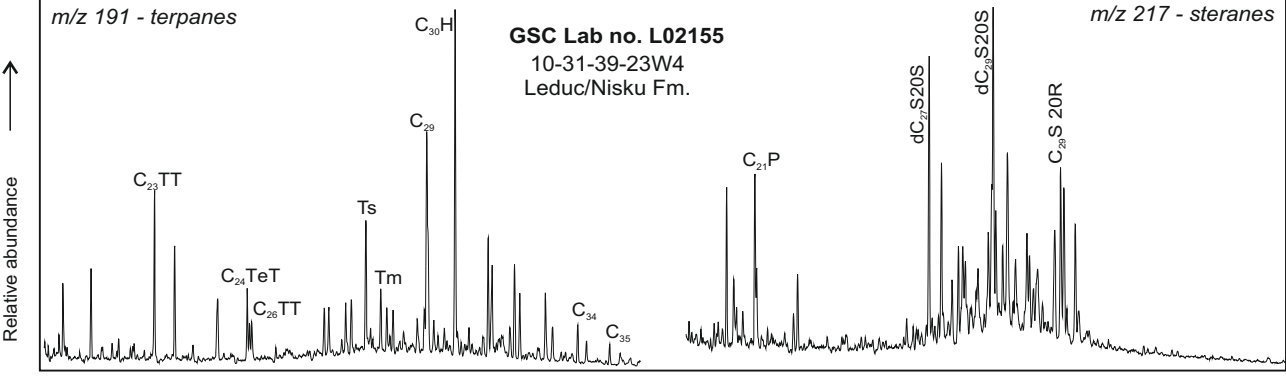
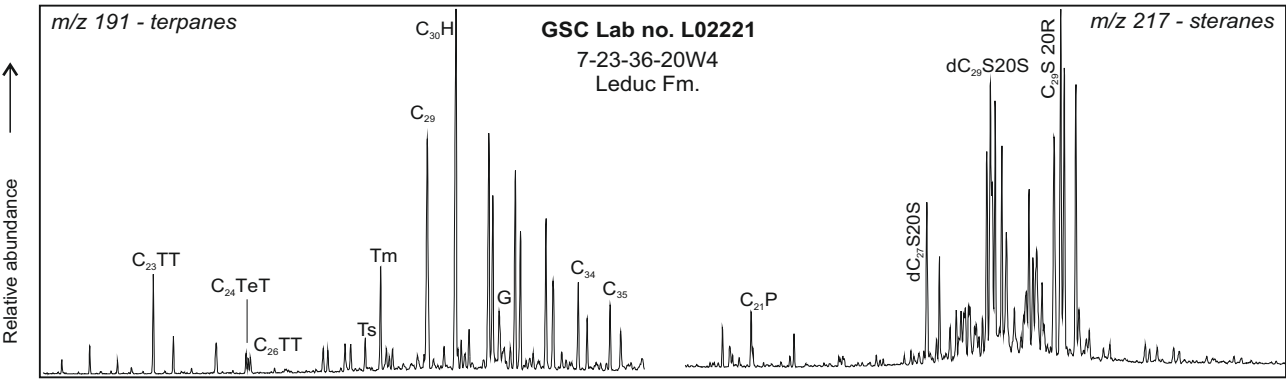


Figure 8b

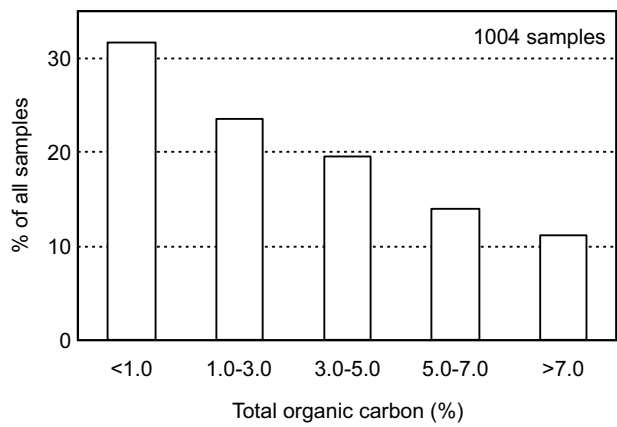


Figure 9

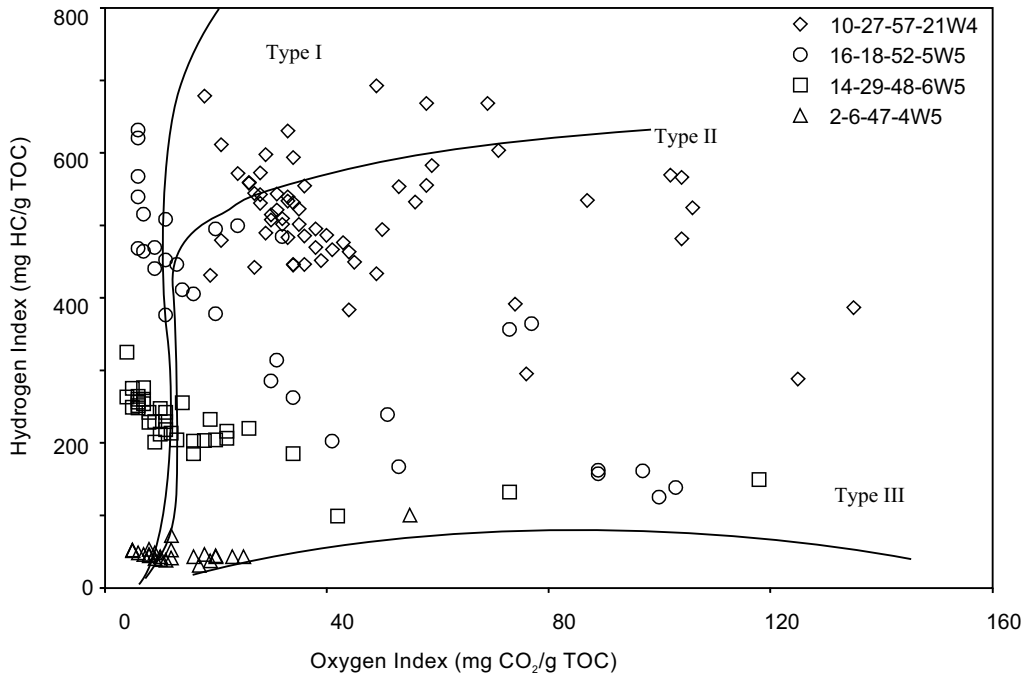


Figure 10

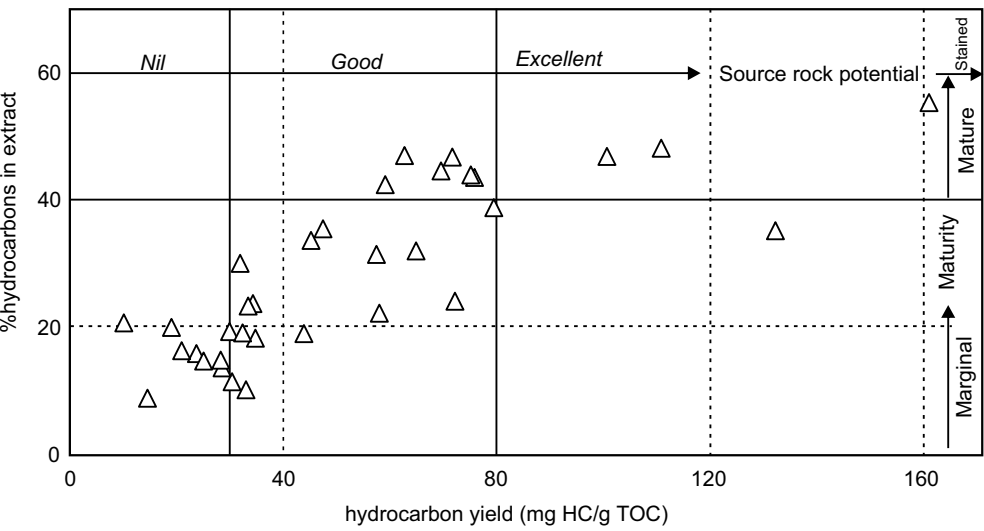


Figure 11

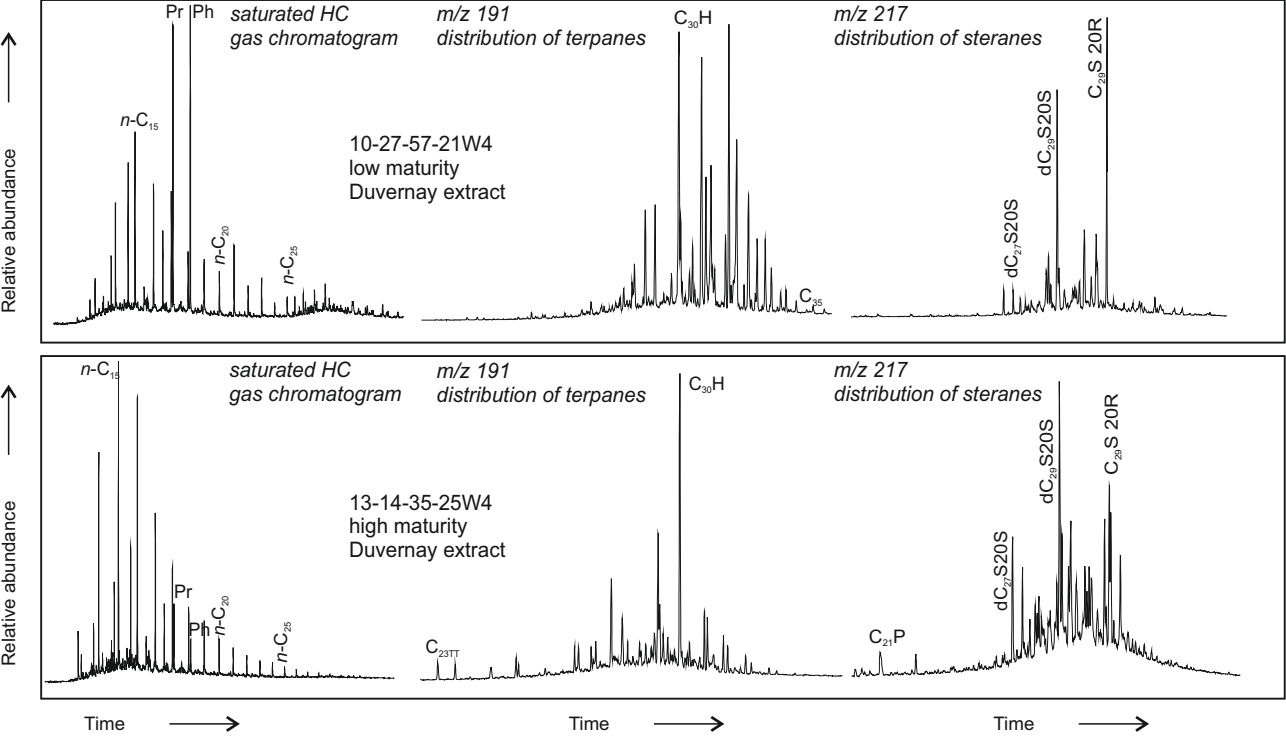


Figure 12

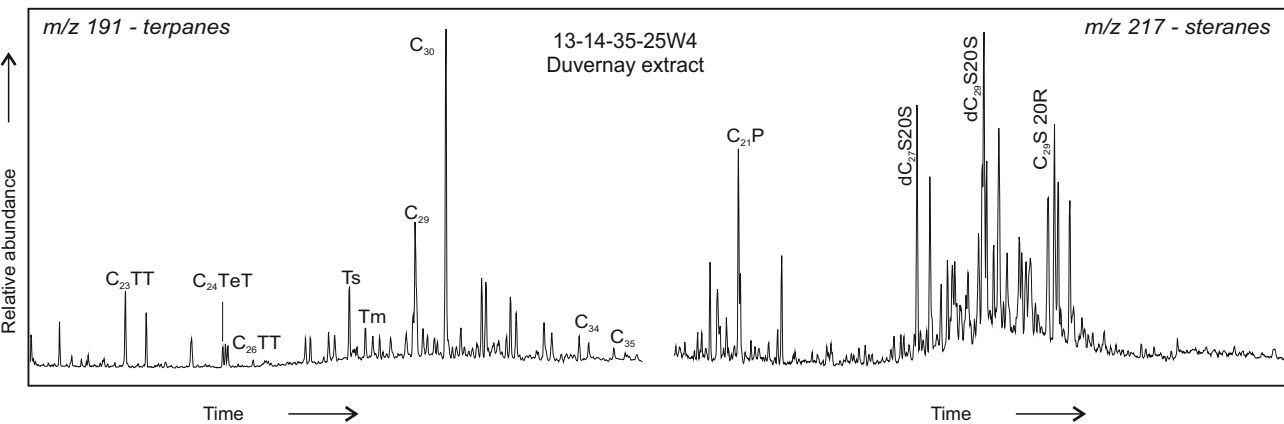
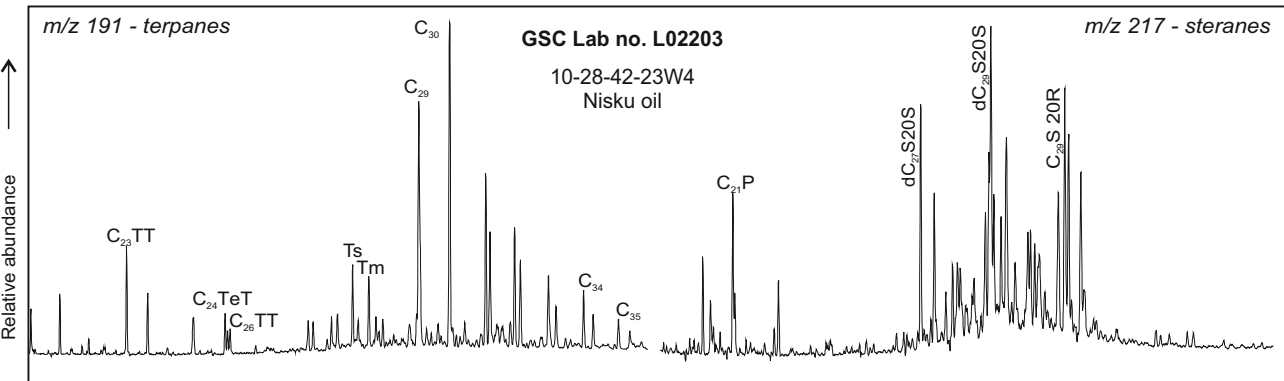


Figure 13

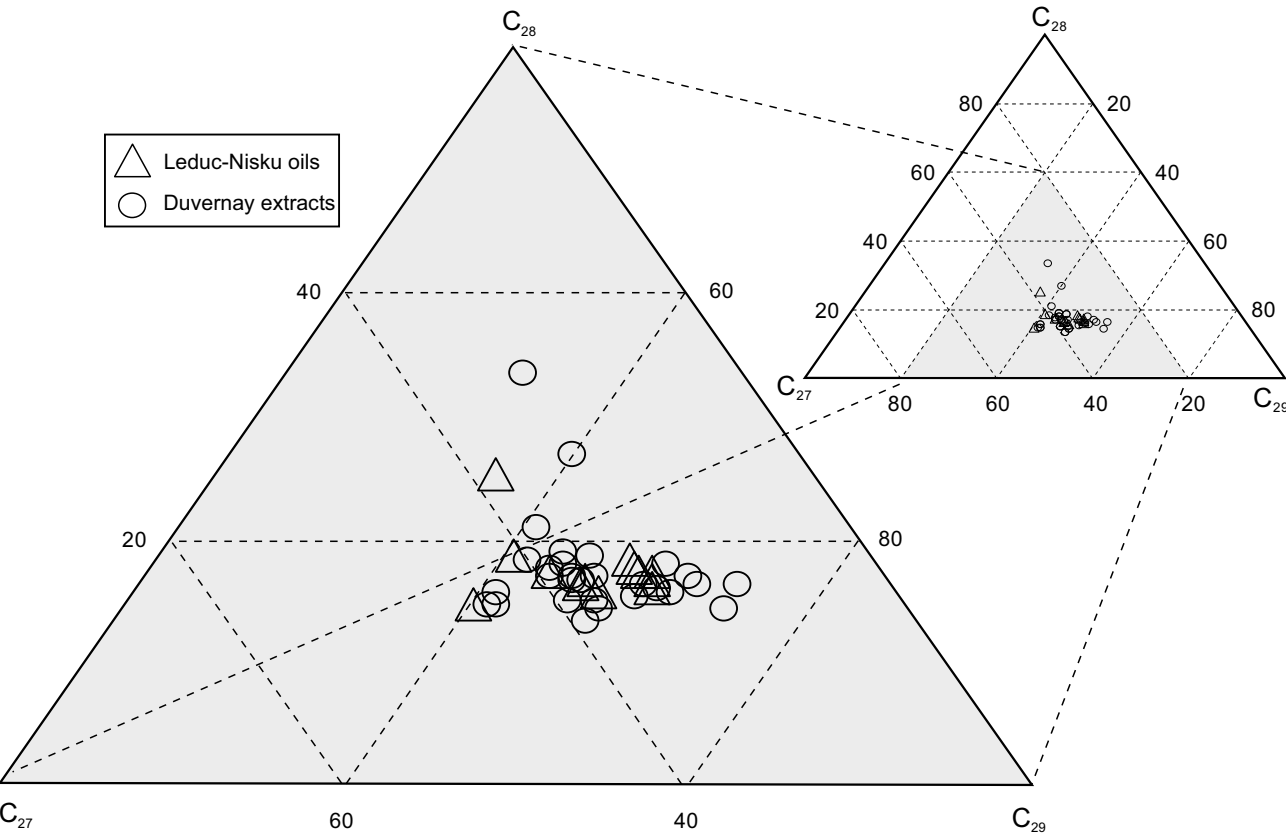


Figure 14

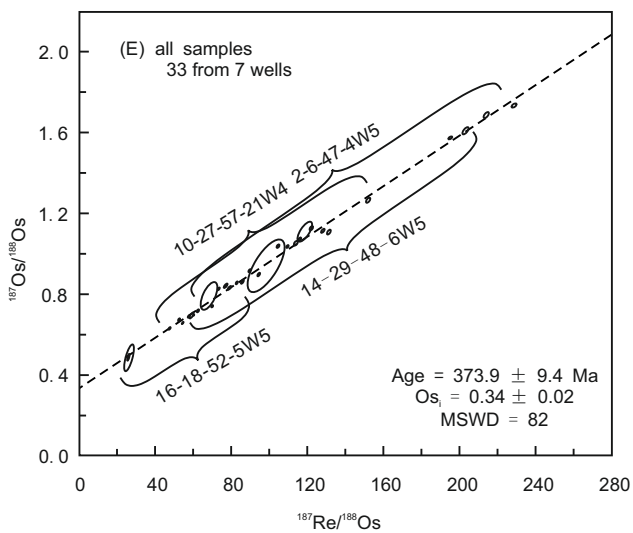
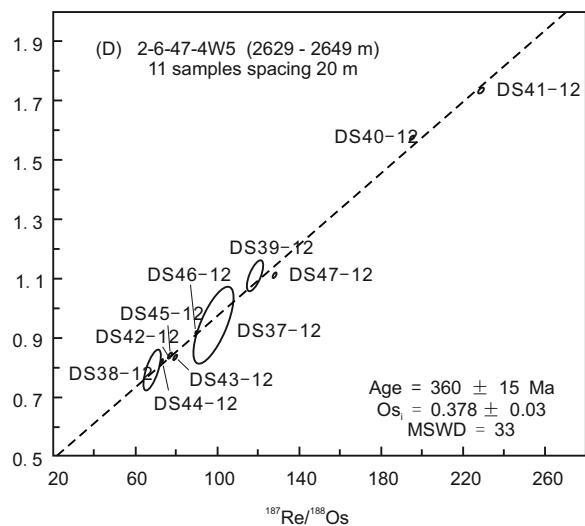
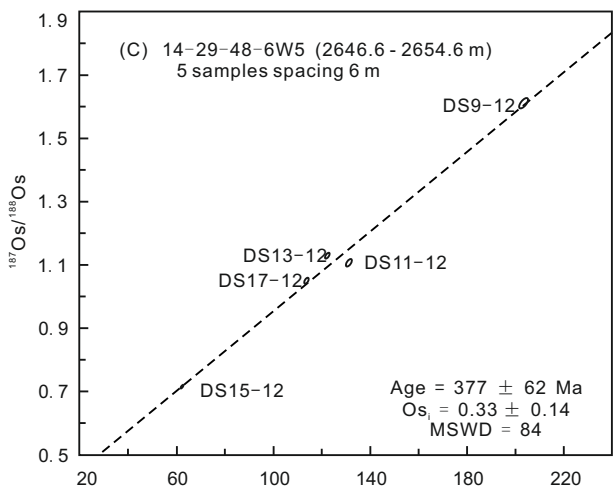
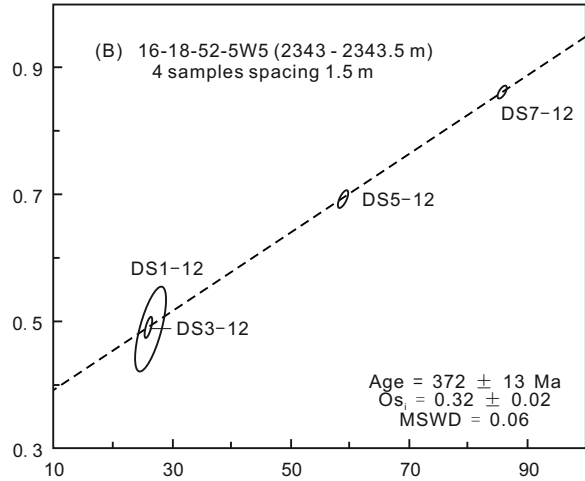
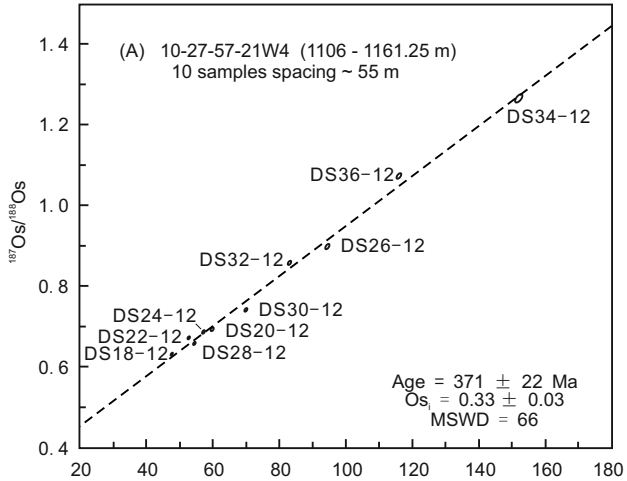


Figure 15

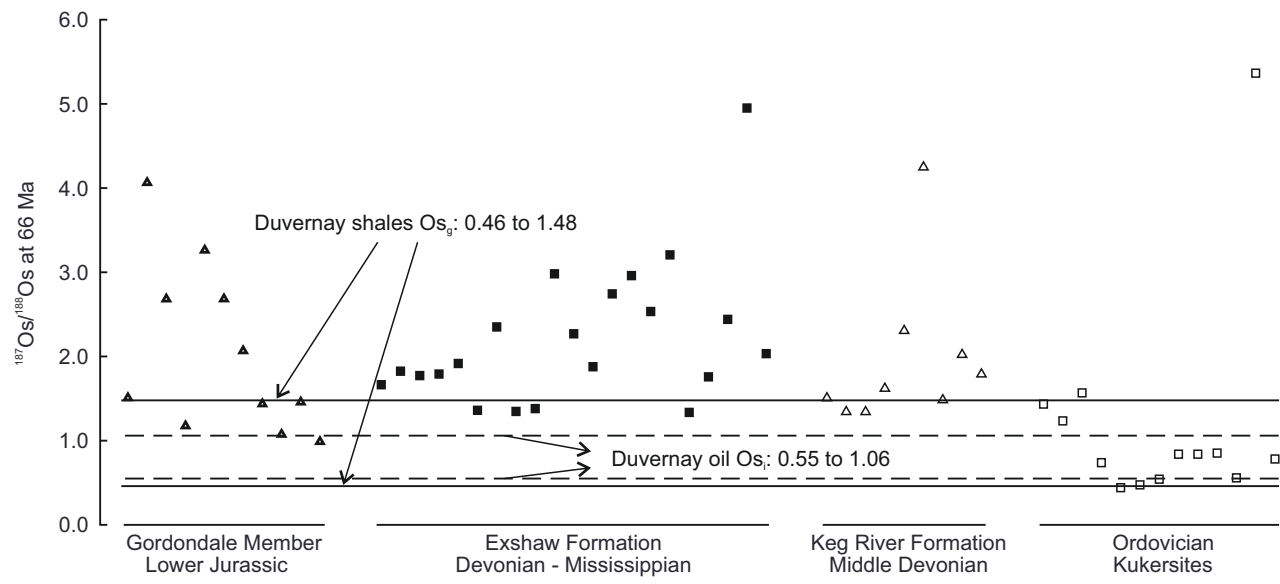


Figure 16